TITLE

An important role for triglyceride in regulating spermatogenesis

AUTHORS

Charlotte F. Chao[1&], Yanina-Yasmin Pesch[1&], Huaxu Yu[2], Chenjingyi Wang[2], Maria Aristizabal[3], Tao Huan[2], Guy Tanentzapf[1], Elizabeth J. Rideout[1*]

AFFILIATIONS

[1] Department of Cellular and Physiological Sciences, Life Sciences Institute, The University of British Columbia, Vancouver, BC, Canada V6T 1Z3

[2] Department of Chemistry, The University of British Columbia, Vancouver, BC, Canada V6T 1Z1

[3] Department of Biology, Queen's University, Kingston, ON, Canada K7L 3N6

* Corresponding author

[&] Equally contributing authors

[*] Correspondence: elizabeth.rideout@ubc.ca

ABSTRACT

Drosophila is a powerful model to study how lipids affect spermatogenesis. Yet, the contribution of neutral lipids, a major lipid group which resides in organelles called lipid droplets (LD), to normal sperm development is largely unknown. Emerging evidence suggests that LD are present in the testis and that loss of neutral lipid- and LD-associated genes causes subfertility; however, key regulators of testis neutral lipids and LD remain unclear. Here, we show that LD are present in early-stage somatic and germline cells within the *Drosophila* testis. We identified a role for triglyceride lipase *brummer* (*bmm*) in regulating testis LD, and found that whole-body loss of *bmm* leads to defects in sperm development. Importantly, these represent cell-autonomous roles for *bmm* in regulating testis LD and spermatogenesis. Because lipidomic analysis of *bmm* mutants revealed excess triglyceride accumulation, and spermatogenic defects in *bmm* mutants were rescued by genetically blocking triglyceride synthesis, our data suggest that *bmm*-mediated regulation of triglyceride influences sperm development. This identifies triglyceride as an important neutral lipid that contributes to *Drosophila* sperm development, and reveals a key role for *bmm* in regulating testis triglyceride levels during spermatogenesis.

35 **KEYWORDS**

36 Triglyceride, lipid droplet, spermatogenesis, testis, *brummer*, adipose triglyceride lipase

37 (ATGL), lipidomics.

38

INTRODUCTION

Lipids play an essential role in regulating spermatogenesis across animals [1–4]. Studies in *Drosophila* have illuminated key roles for multiple lipid species in regulating sperm development [5–7]. For example, phosphatidylinositol and its phosphorylated derivatives participate in diverse aspects of *Drosophila* spermatogenesis including meiotic cytokinesis [1,8–11], somatic cell differentiation [12], germline and somatic cell polarity maintenance [13–16], and germline stem cell (GSC) maintenance and proliferation [17]. Membrane lipids also influence sperm development [18,19], whereas fatty acids play a role in processes such as meiotic cytokinesis [20] and sperm individualization [21,22]. While these studies suggest key roles for membrane lipids and fatty acids during *Drosophila* spermatogenesis, some of which are conserved in mammals [23–25], much less is known about how neutral lipids contribute to spermatogenesis.

Neutral lipids are a major lipid group that includes triglyceride and cholesterol ester, and reside within specialized organelles called lipid droplets (LD) [26]. LD are found in diverse cell types (*e.g*. adipocytes, muscle, liver, glia, neurons) [27,28,26], and play key roles in maintaining cellular lipid homeostasis. In nongonadal cell types, correct regulation of LD contributes to cellular energy production [29–31], sequestration and redistribution of lipid precursors [32–36], and regulation of lipid toxicity [37–39]. The importance of LD to normal cellular function in nongonadal cell types is shown by the fact that dysregulation of LD causes defects in cell differentiation, survival, and energy production [26,37,40,41]. In the testis, much less is known about the regulation and function of neutral lipids and LD, and how this regulation affects sperm development.

Multiple lines of evidence suggest a potential role for neutral lipids and LD during spermatogenesis. First, genes that encode proteins associated with neutral lipid metabolism and LD are expressed in the testis across multiple species [42–44]. Second, testis LD have been identified in mammals and flies under both normal physiological conditions [27,44–48] and after mitochondrial stress [49]. Third, loss of genes associated with neutral lipid metabolism and LD cause subfertility phenotypes in both flies and mammals [27,50–52]. While studies suggest that mammalian testis LD contribute to steroidogenesis [53,54], the spatial, temporal, and cell-type specific requirements for neutral lipids and LD in the testis have not been explored in detail in any animal. It remains similarly unclear which genes are responsible for regulating neutral lipids and LD during spermatogenesis.

To address these knowledge gaps, we used *Drosophila* to investigate the regulation and function of neutral lipids and LD during sperm development. Our detailed analysis of spermatogenesis under normal physiological conditions revealed the presence of LD in early-stage somatic and germline cells in the testis. We identified triglyceride lipase *brummer* (*bmm*) as a regulator of testis LD, and showed that this represents a cell-autonomous role for *bmm*. Importantly, we found that the *bmm*-mediated regulation of testis LD was significant for spermatogenesis, as both whole-body and cell-autonomous loss of *bmm* caused defects in sperm development. Given that our lipidomic analysis revealed an excess accumulation of triglyceride in animals lacking *bmm*, and that genetically blocking triglyceride synthesis rescued many spermatogenic defects associated with *bmm* loss, our data suggests that *bmm*-mediated regulation of triglyceride is important for normal *Drosophila* sperm

development. This reveals previously unrecognized roles for neutral lipids such as triglyceride in regulating spermatogenesis, and for *bmm* in regulating sperm development under normal physiological conditions. Together, these findings advance knowledge of the regulation and function of neutral lipids during spermatogenesis.

RESULTS

Lipid droplets are present in early-stage somatic and germline cells

We previously reported the presence of small circular punctae (<1 μm) corresponding to LD near the apical tip of the testis [27]. We confirm these results in w^{1118} males using neutral lipid stain BODIPY (4,4-Difluoro-1,3,5,7,8-Pentamethyl-4-Bora-3a,4a-Diaza-*s*-Indacene) (Figure 1A). Importantly, we reproduced this spatial distribution of LD in two independent genetic backgrounds and at two additional ages (Figure 1B,1C). In all cases, LD were in a testis region that contains stem cells and early-stage somatic and germline cells (Figure 1A-A', arrows), and in the hub, an organizing center and stem cell niche in the *Drosophila* testis (Figure 1A''-A''', arrows) [55]. LD were largely absent from the testis region occupied by spermatocytes (Figure 1A and A', arrowheads). While LD may contain multiple neutral lipid species[56], cholesterol-binding fluorescent polyene antibiotic filipin III did not detect cholesterol within testis LD (Figure S1A), suggesting triglyceride is the main neutral lipid in *Drosophila* testis LD.

Drosophila spermatogenesis requires the codevelopment and differentiation of two cell lineages, the germline and the somatic cells [57]. To identify LD in each lineage, we used the GAL4/UAS system to overexpress a transgene in which GFP is fused to the LD-targeting motif of motor protein Klarsicht [58] (*UAS-GFP-LD*). We targeted *UAS-*

GFP-LD to somatic cells with *Traffic jam* (*Tj*)-*GAL4* and to the germline using *nanos (nos)-GAL4*; LD were visualized using neutral lipid dye LipidTox. We found LD in the somatic cells of 0-day-old males (Figure 1D), and showed that the majority of somatic LD were <30 μm from the hub (Figure 1E). Because the somatic LD distribution coincided with a marker for somatic stem cells and their immediate daughter cells (Zinc finger homeodomain 1, Zfh-1) (Figure 1F; two-sample Kolmogorov-Smirnov test) [59], but not with a marker for late somatic cells (Eyes absent, Eya) [12,60], our data suggests LD are present in early somatic cells. In the germline, GFP punctae corresponding to LD were found near the apical tip of the testis in 0-day-old males (Figure 1G,H). We found that the disappearance of germline LD coincided with peak expression of a GFP reporter that reflects the expression of Bag-of-marbles (Bam) protein in the testis (Bam-GFP) [61] (Figure 1I,1J). Because peak Bam expression signals the last round of transient amplifying mitotic cell cycle prior to the germline's transition into the meiotic cell cycle [62–64], our data suggests that germline LD, like somatic LD, are present at early stages of germline development.

brummer plays a cell-autonomous role in regulating testis lipid droplets

Adipose triglyceride lipase (*ATGL*) is a critical regulator of neutral lipid metabolism and LD [65–74]. Loss of *ATGL* in many cell types triggers LD accumulation, and *ATGL* overexpression decreases LD number [30,67,68,71,73,73,75,76]. Given that the *Drosophila ATGL* homolog *brummer* (*bmm*) regulates testis LD induced by mitochondrial stress [49], we explored whether *bmm* regulates testis LD under normal physiological conditions. We first examined *bmm* expression in the testis by isolating

this organ from flies in which a *bmm* promoter fragment drives *GFP* expression (*bmm-GFP*). Indeed, *bmm-GFP* accurately reproduces changes to *bmm* mRNA levels [77]. GFP expression was present in the germline of *bmm-GFP* testes, and we found germline GFP levels were higher in spermatocytes than at earlier stages of sperm development (Figure 2A,2B; one-way ANOVA with Tukey multiple comparison test). Supporting this, our analysis of a publicly available single-cell RNA sequencing data set of the male reproductive organ [78] suggested a similar trend in *bmm* mRNA levels between different stages of germline (Figure S2A,S2B) and somatic cell (Figure S2C,S2D) development. Importantly, germline GFP levels were negatively correlated with testis LD in *bmm-GFP* flies (Figure 2A,2C), suggesting regions with higher *bmm* expression had fewer LD.

To test whether *bmm* regulates testis LD, we compared LD in testes from 0-day-old males carrying a loss-of-function mutation in *bmm* (bmm^{1}) to control male testes (bmm^{rev})[67]. bmm^{1} testes had significantly more LD across all LD sizes compared with control males (Figure 2D–2G; Welch two-sample t-test with Bonferroni correction), and showed a significantly expanded LD distribution (Figure 2D–2F,2H; two-sample Kolmogorov-Smirnov test). This suggests *bmm* normally restricts LD to the region near the apical tip of the testis, a role we confirm in both somatic and germline lineages (Figure S2E–S2H). Importantly, after inducing homozygous bmm^{1} or bmm^{rev} clones in the testes using *FLP-FRT* system[79], we found bmm^{1} spermatocyte clones had significantly more LD at 3 days post-clone induction (Figure 2I; Welch two-sample t-test), a stage at which LD were absent from bmm^{rev} clones. This indicates a previously

unrecognized cell-autonomous role for *bmm* in regulating testis LD, a role we were unable to assess in somatic cells as we recovered no bmm^{1} somatic cell clones.

brummer **plays a cell-autonomous role in regulating germline development**

To determine the physiological significance of *bmm*-mediated regulation of testis LD, we investigated testis and sperm development in males without *bmm* function. In 0-day-old bmm^{1} males reared at 25°C, testis size was significantly smaller than in age-matched bmm^{rev} controls (Figure S3A; Welch two-sample t-test), and the number of spermatid bundles was significantly lower (Figure S3B; Kruskal-Wallis rank sum test). Defects in testis size and sperm development were also observed in 14-day-old bmm^{1} males (Figure S3C,S3D Welch two-sample t-test). When the animals were reared at 29°C, a temperature that exacerbates spermatogenesis defects associated with changes in lipid metabolism [21], bmm^{1} phenotypes were more pronounced (Figure 3A-3C). This suggests loss of *bmm* affects testis development and spermatogenesis. Because similar phenotypes are observed in male mice without ATGL [52], and supplementing the diet of bmm^{1} males with medium-chain triglycerides (MCT) partially rescues the testis and spermatogenic defects we observed in flies (Figure S3E,S3F; one-way ANOVA with Tukey multiple comparison test), as it does in mice [52,80], our data suggests flies are a good model to study how *bmm*/*ATGL* influences sperm development.

To explore spermatogenesis in bmm^{1} animals, we used germline-specific marker Vasa to visualize the germline in the testes of bmm^{1} and bmm^{rev} males (Figure 3D,3E) [81]. We observed a significant increase in the number of germline stem cells (GSC) (Figure 3F; Kruskal-Wallis rank sum test) and higher variability in GSC number in bmm^{1}

176 males (p=5.7×10^{-12} by F-test). Given that GSC number is affected by hub size and GSC
177 proliferation [82,83], we monitored both parameters in *bmm^{1}* and *bmm^{rev}* controls. While
178 hub size in *bmm^{1}* testes was significantly larger than in testes from *bmm^{rev}* controls
179 (Figure S3G,S3H; Welch two-sample t-test), the number of phosphohistone H3-positive
180 GSC, which indicates proliferating GSC, was unchanged in *bmm^{1}* animals (Figure S3I;
181 Kruskal-Wallis rank sum test). While this indicates a larger hub may partly explain
182 *bmm's* effect on GSC number, *bmm* also plays a cell-autonomous role in regulating
183 GSC, as we recovered a higher proportion of *bmm^{1}* clones in the GSC pool compared
184 with *bmm^{rev}* clones at 14 days after clone induction (Figure 3G; Welch two-sample t-
185 test).

186 Beyond GSC, we uncovered additional spermatogenesis defects in *bmm^{1}* testes.
187 Peak Bam-GFP expression in testes from 0-day-old *bmm^{1}* and *bmm^{rev}* males showed
188 that GFP-positive cysts with were significantly further away from the hub in *bmm^{1}* testes
189 (Figure 3H,S3J; Welch two-sample t-test). Indeed, 15/18 *bmm^{1}* testes contained Vasa-
190 positive cysts with large nuclei in the distal half of the testis (Figure 3I, arrowheads), a
191 phenotype not present in *bmm^{rev}* testes (0/8) (p=0.0005 by Pearson's Chi-square test).
192 Because these phenotypes are also seen in testes with differentiation defects [13,84],
193 we recorded the stage of sperm development reached by the germline in *bmm^{1}* testes.
194 Most *bmm^{1}* testes contained post-meiotic cells in males raised at 25°C (Figure S3K);
195 however, germline development did not progress past the spermatocyte stage in most
196 *bmm^{1}* testes from animals raised at 29°C (Figure S3K). Testes from *bmm^{1}* males reared
197 at 25°C also had a smaller Boule-positive area (Figure 3J,S3L; Welch two-sample t-
198 test), and fewer individualization complexes and waste bags (Figure S3M,S3N; Kruskal-

Wallis rank sum test). Together, these data indicate loss of *bmm* delays germline development. Because we recovered fewer bmm^{1} spermatocyte and spermatid clones 14 days after clone induction (Figure 3K,3L; Kruskal-Wallis rank sum test), this effect on germline development represents a cell-autonomous role for *bmm*.

***brummer*-dependent regulation of testis triglyceride levels affects spermatogenesis**

ATGL catalyzes the first and rate-limiting step of triglyceride hydrolysis [73,85,86]. Loss of this enzyme or its homologs leads to excess triglyceride accumulation [27,30,67,73,75] and shifts in multiple lipid classes [66,87–89]. To determine how loss of *bmm* affects spermatogenesis, we carried out mass spectrometry (MS)-based untargeted lipidomic profiling of bmm^{1} and bmm^{rev} males. Hierarchical clustering of lipid species suggests that bmm^{1} and bmm^{rev} males show distinct lipidomic profiles (Figure 4A). Overall, we detected 2464 and 1144 lipid features with high quantitative confidence in positive and negative ion modes, respectively. By matching experimental *m/z*, isotopic ratio, and tandem MS spectra to lipid libraries, we confirmed 293 unique lipid species (Supplemental table 1). We found 107 lipids had a significant change in abundance between bmm^{1} and bmm^{rev} males ($p_{adj}<0.05$): 85 species were upregulated in bmm^{1} males and 22 lipid species were downregulated. Among differentially regulated species from different lipid classes, triglyceride had the largest residual above expected proportion ($p=5.00\times10^{-4}$ by Pearson's Chi-squared test). This suggests triglyceride is the lipid class most affected by loss of *bmm* (Figure 4B,4C).

In *bmm*^{1} males, most triglyceride species (55/97) were significantly higher. Because we observed a positive correlation between the fold increase in triglyceride abundance with both the number of double bonds (p=7.52×10^{-8} by Kendall's rank correlation test; Figure S4A) and the number of carbons (p=2.77×10^{-10} by Kendall's rank correlation test; Figure S4B), our data align well with *bmm*/*ATGL's* known role in regulating triglyceride levels[67,68,73] and its substrate preference of long-chain polyunsaturated fatty acids[85]. While we also detected changes in species such as fatty acids, acylcarnitine, and membrane lipids (Figure S4C–S4H), in line with recent *Drosophila* lipidomic data[90,91], the striking accumulation of triglyceride in *bmm*^{1} males suggested that excess testis triglyceride in *bmm*^{1} males may contribute to their spermatogenic defects. To test this, we examined spermatogenesis in *bmm*^{1} males carrying loss-of-function mutations in *midway* (*mdy*). *mdy* is the *Drosophila* homolog of *diacylglycerol O-acyltransferase 1* (*DGAT1*), and whole-body loss of *mdy* reduces whole-body triglyceride levels[92–94]. Importantly, testes isolated from males lacking both *bmm* and *mdy* (genotype *mdy*$^{QX25/k03902}$*;bmm*^{1}) had fewer LD than testes dissected from *bmm*^{1} males (Figures 4D,S4I; one-way ANOVA with Tukey multiple comparison test).

We found that testes isolated from *mdy*$^{QX25/k03902}$*;bmm*^{1} males were significantly larger and had more spermatid bundles than testes from *bmm*^{1} males (Figure 4E–G; one-way ANOVA with Tukey multiple comparison test). The elevated number of GSC in *bmm*^{1} male testes was similarly rescued in *mdy*$^{QX25/k03902}$*;bmm*^{1} males (Figure 4H; one-way ANOVA with Tukey multiple comparison test). These data suggest that defective spermatogenesis in *bmm*^{1} males can be partly attributed to excess triglyceride

accumulation. Notably, at least some of these defects are cell-autonomous: RNAi-mediated knockdown of *mdy* in the germline of *bmm*^{1} males partially rescued the defects in testis size (Figure 4I; Kruskal-Wallis rank sum test with Dunn's multiple comparison test) and GSC variance (Figure S4J; p=4.5 x 10^{-5} and 8.2 x 10^{-3} by F-test from the GAL4- and UAS-only crosses, respectively). *bmm*-mediated regulation of testis triglyceride therefore plays a previously unrecognized role in regulating sperm development.

DISCUSSION

In this study, we used *Drosophila* to gain insight into how the neutral lipids, a major lipid class, contribute to sperm development. We describe the distribution of LD under normal physiological conditions in the *Drosophila* testis, and show that LD are present at the early stages of development in both somatic and germline cells. While many factors are known to regulate LD in nongonadal cell types, we reveal a cell-autonomous role for triglyceride lipase *bmm* in regulating testis LD during spermatogenesis. Indeed, our data indicates loss of *bmm* delays germline differentiation leading to an accumulation of early-stage germ cells. These defects in germline differentiation can be partially explained by the excess accumulation of triglyceride in flies lacking *bmm*, as genetically blocking triglyceride synthesis rescues multiple spermatogenic defects in *bmm* mutants. Together, our data reveals previously unrecognized roles for LD and triglycerides during spermatogenesis, and for *bmm* as an important regulator of testis LD and germline development under normal physiological conditions.

One key outcome of our study was increased knowledge of LD regulation and function in the testis. Despite rapidly expanding knowledge of LD in cell types such as adipocytes or skeletal muscle, less is known about how LD influence spermatogenesis under normal physiological conditions. In mammals, testis LD contain cholesterol and play a role in promoting steroidogenesis [95,96]. In flies, we show that LD are present in the testis, and that excess accumulation of these LD affects sperm development. In nongonadal cell types, triglycerides provide a rich source of fatty acids for cellular ATP production, lipid building blocks to support membrane homeostasis and growth, and metabolites that can act as signaling molecules [26]. Because ATP production, lipid precursors, and lipid signaling all play roles in supporting normal sperm development [97,98], future studies will need to determine how each of these processes is affected when excess triglyceride accumulates in testis LD. This will provide critical insight into how triglyceride stored within testis LD contributes to overall cellular lipid metabolism during spermatogenesis. Because of the parallel spermatogenic defects we observed in *bmm* mutants and *ATGL*-deficient mice, we expect that these mechanisms will also operate in other species.

A more comprehensive understanding of neutral lipid metabolism during sperm development will also emerge from studies on the upstream signaling networks that regulate testis LD and triglyceride. Given that we show an important and cell-autonomous role for *bmm* in regulating testis LD and triglyceride, future studies will need to identify factors that regulate *bmm* in the testis. Based on public single-cell RNAseq data and the *bmm-GFP* reporter strain, our data suggest *bmm* mRNA levels are differentially regulated between early and later stages of sperm development.

Candidates for mediating this regulation include the insulin/insulin-like growth factor signaling pathway (IIS), Target of rapamycin (TOR) pathway, and nuclear factor κB/Relish pathway (NFκB), as all of these pathways influence *bmm* mRNA levels in nongonadal cell types [99–105]. Beyond mRNA levels, Bmm protein levels and post-translational modifications may also be differentially regulating during spermatogenesis. For example, studies show that the proteins encoded by *bmm* homologs in other animals are regulated by phosphorylation [106], mediated by kinases such as adenosine monophosphate-activated protein kinase (AMPK) and protein kinase A (PKA) [107–109]. Importantly, many of these pathways, including IIS, TOR, AMPK, NFκB and possibly PKA influence *Drosophila* sperm development [110–115]. Identifying the signaling networks that influence *bmm* regulation during sperm development will therefore lead to a deeper understanding of how testis LD and triglyceride are coordinated with physiological factors to promote normal spermatogenesis. Because pathways such as IIS and AMPK, and others, regulate sperm development in other species [116–118], these insights may reveal conserved mechanisms that govern the regulation of cellular neutral lipid metabolism during sperm development.

ACKNOWLEDGEMENTS

We thank Dr. Ronald Kühnlein for *bmm*^{1} and *bmm*^{rev} lines [67], Dr. Michael Welte for *UAS-GFP-LD*[58], and Dr. Kaeko Kamei for *bmm-GFP* [77]. We used stocks from the Bloomington *Drosophila* Stock Center (NIH P40OD018537) and Vienna *Drosophila* Resource Center (VDRC). We acknowledge critical resources and information provided by FlyBase [119] (supported by the National Human Genome Research Institute at the U.S. National Institutes of Health (U41 HG000739) and the British Medical Research Council (MR/N030117/1)). This work was supported by the Life Sciences Institutes Imaging Core, supported by the UBC GREx Biological Resilience Initiative. Funding for this study was provided by grants to EJR from the Canadian Institutes for Health Research (PJT-153072), Michael Smith Foundation for Health Research (16876), and the Canadian Foundation for Innovation (JELF-34879). GT was supported by a grant from the Natural Sciences and Engineering Research Council (NSERC; 2018-04648), TH/HY/CW were supported by NSERC (2020-04895), MA was supported by the Jacob's foundation. We would like to acknowledge that our research takes place on the traditional, ancestral, and unceded territory of the Musqueam people; a privilege for which we are grateful.

AUTHOR CONTRIBUTIONS

Conceptualization, C.C. and E.J.R.; Methodology, C.C. and Y.Y.P.; Software, C.C.; Investigation, C.C., H.Y., and Y.Y.P.; Lipidomics, M.A., H.Y., C.W., T.H.; Writing – Original Draft, C.C. and E.J.R.; Writing – Review and Editing, C.C., E.J.R., and Y.Y.P.;

Supervision, E.J.R., G.T., and T.H.; Project administration, E.J.R.; Funding Acquisition, E.J.R., G.T., and T.H.

DECLARATION OF INTERESTS

The authors declare no competing interests.

FIGURE LEGENDS

Figure 1 – Lipid droplets are present in early-stage somatic and germ cells. (A) Testis lipid droplets (LD) in w^{1118} animals visualized with neutral lipid dye BODIPY. (A,A') Scale bar=50 μm; (A'',A''') scale bar=15 μm. Asterisk indicates hub in all images. Arrows point to LD; arrowheads point to spermatocytes in A,B. (B) Testis LD visualized with BODIPY in newly-eclosed males from two wild-type genotypes. Scale bars: main image=50 μm; inset image=10 μm. (C) Testis LD from w^{1118} animals at different times post-eclosion. Scale bars=50 μm. (D) Testis LD visualized with LipidTox Red in animals with somatic cell overexpression of GFP-LD (*Tj-GAL4>UAS-GFP-LD*). GFP- and LipidTox Red-positive punctae are somatic LD (D–D'' arrows); LipidTox punctae without GFP indicate germline LD (D–D'' arrowheads). Scale bars=10 μm. (E) Histogram showing the spatial distribution of somatic cell LD; error bars represent standard error of the mean (SEM). (F) Cumulative frequency distributions of somatic LD (blue line, data reproduced from E), zfh-1-positive somatic cells (zfh-1$^+$ cells, orange line), and Eya-positive somatic cells (Eya$^+$ cells, grey line). (G) Testis LD visualized with LipidTox Red in males with germline overexpression of GFP-LD (*nos-GAL4>UAS-GFP-LD*). GFP- and LipidTox Red-positive punctae indicate germline LD (arrows); LipidTox punctae without

GFP indicate non-germline LD (arrowheads). Scale bars=10 μm. (H) Histogram representing the spatial distribution of LD within the germline; error bars represent SEM. (I) Histogram representing the spatial distribution of LD and GFP fluorescence (green line) (arbitrary units, a.u.) in a representative testis of a *bam-GFP* animal (panel J). (J) Testis LD in a *bam-GFP* animal; arrows point to LD and arrowheads point to spermatocytes. Scale bar=50 μm. See also Supplemental Figure 1.

Figure 2 – *bmm* regulates testis lipid droplets in a cell-autonomous manner. (A) Testis lipid droplets (LD) indicated by LipidTox Red in *bmm-GFP* animals. Arrows point to LD in all images. Arrowheads point to spermatocytes. Scale bars=50 μm. Asterisks indicate the hub in all images. (B) Quantification of nuclear GFP intensity in testes isolated from *bmm-GFP* animals (n=3). Germline stem cell (GSC), spermatogonia (SG), spermatocyte (SC). (C) Spatial distribution of LD (grey histogram) and GFP expression (green line) in testes from *bmm-GFP* animals as a function of distance from the hub (n=3). (D,E) LD near the apical region of the testis in bmm^{rev} (D) or bmm^{1} (E) animals. (F) LD further away from the apical tip in bmm^{1} animals. (D–F) Scale bars=50 μm. (G) Histogram representing testis LD size distribution in bmm^{rev} (grey) and bmm^{1} (orange). (H) Apical tip of the testes is at the left of the graph; individual dots represent a single LD and its relative position to the hub marked by an asterisk. Cumulative frequency distribution of the distance between LDs and the apical tip of the testes are drawn as solid lines. (I) Number of testis LD in bmm^{rev} (grey) or bmm^{1} (orange) in FLP-FRT clones 3 days post-clone induction; dots represent measurements from a single clone.

The number of cells in each cyst (CC) counted is indicated. See also Supplemental Figure 2.

Figure 3 – A cell-autonomous role for *bmm* in regulating spermatogenesis. Testes isolated from bmm^{rev} (A) and bmm^{1} (A') animals raised at 29°C stained with phalloidin. Scale bars=100 μm. (B) Testis size in bmm^{1} and bmm^{rev} animals raised at 29°C. (C) Spermatid bundle number in bmm^{1} and bmm^{rev} testes from animals reared at 29°C. (D,E) Representative images of bmm^{rev} (D) or bmm^{1} (E) testes stained with DAPI and anti-Vasa antibody. Arrows indicate germline stem cells (GSC). Scale bar=50 μm. The hub is marked by an asterisk in all images. (F) GSC number in bmm^{1} and bmm^{rev} testes. (G) Proportion of GSCs that were either bmm^{1} or bmm^{rev} clones at 3 and 14 days post-clone induction. (H) Representative images of bmm^{rev} (H) and bmm^{1} (H') testes carrying *bam-GFP*; data quantified in Figure S3J. Arrows indicate regions with high Bam-GFP. Scale bars=50 μm. (I) Representative images of bmm^{rev} (I) or bmm^{1} (I',I'') testes stained with anti-Vasa antibody. Arrows indicate Vasa-positive cysts in bmm^{1} testis. Panel I'' is magnified from the boxed region in I'. (I,I') Scale bars=100 μm; (I'') scale bar=50 μm. (J) Maximum projection of bmm^{rev} (J) or bmm^{1} (J') testes stained with anti-Boule antibody (green) and DAPI (blue). Scale bars=100 μm. Number of bmm^{1} and bmm^{rev} spermatocyte clones (K) or post-meiotic clones (L) at 3 and 14 days post-clone induction. See also Supplemental Figure 3.

Figure 4 – Loss of *bmm* disrupts triglyceride homeostasis and leads to spermatogenic defects. (A) Hierarchical clustering of lipid species detected in bmm^{rev}

and *bmm*^{1} animals. (B) Histograms showing the proportion of species in each lipid class with different levels between *bmm*^{1} and *bmm*^{rev}. Numbers on histograms indicate the number of species with differences in abundance. (C) Volcano plot showing fold change in abundance of triglycerides (green; 97 species) and non-triglyceride lipids (grey; 186 species) in our dataset. (D) Arrows indicate testis LD stained with LipidTox Red in *bmm*^{rev} (D), *bmm*^{1} (D'), or *mdy*$^{QX25/k03902}$; *bmm*^{1} (D'') animals. (E) Whole testes isolated from *bmm*^{rev} (E), *bmm*^{1} (E'), or *mdy*$^{QX25/k03902}$;*bmm*^{1} (E'') animals stained with anti-Vasa antibody (red) and DAPI (blue). Arrowheads indicate spermatid bundles. Scale bars=100 μm. (F) Testis size in *bmm*^{rev}, *bmm*^{1}, and *mdy*$^{QX25/k03902}$;*bmm*^{1} animals. Spermatid bundles (G) and number of germline stem cells (H) in *bmm*^{rev}, *bmm*^{1}, and *mdy*$^{QX25/k03902}$;*bmm*^{1} animals. (I) Testis size in animals with germline-specific *mdy* knockdown (*nos-GAL4>mdy RNAi*; *bmm*^{1}) compared with controls (*nos-GAL4>+*; *bmm*^{1} and *+>mdy RNAi*; *bmm*^{1}). See also Supplemental Figure 4.

MATERIALS AND METHODS

Materials and Resource availability. *Drosophila* strains and their source are listed in a Key Resources table. Further information and requests for resources and reagents should be directed to, and will be fulfilled by, lead contact Dr. Elizabeth J. Rideout (elizabeth.rideout@ubc.ca).

Data and Code availability. All raw data and results of statistical tests reported in this paper are located in Supplementary files 1-4. This paper does not report original code. Any additional information required to reanalyze the data reported in this paper is available from the lead contact upon request.

Fly husbandry. Fly stocks were maintained at room temperature in 12:12 hour light:dark cycle. Unless otherwise indicated, all flies were raised at 25°C with a density of 50 larvae per 10 mL fly media. Because this project examines sperm development, we used male flies in all experiments. Fly media contained 20.5 g sucrose (SU10, Snow Cap), 70.9 g Dextrose (SUG8, Snow Cap), 48.5 g cornmeal (AO18006, Snow Cap), 30.3 g baker's yeast (NB10, Snow Cap), 4.55 g agar (DR-820-25F, SciMart), 0.5 g calcium chloride dihydrate (CCL302.1, BioShop Canada), 0.5 g magnesium sulfate heptahydrate (MAG511.1, BioShop Canada), 4.9 mL propionic acids (P1386, Sigma-Aldrich), and 488 µL phosphoric acid (P5811, Sigma-Aldrich) per 1L of media. For diets with medium- or long-chain triglyceride, 4 g of coconut oil (medium chain triglyceride) or olive oil (long chain triglyceride) was added per 100 mL of media described above prior

436 to cooling. Males were collected and dissected within 24 hours of eclosion unless
437 otherwise indicated. Fixations were performed at room temperature with 4%
438 paraformaldehyde (CA11021-168, VWR) in PBS for 20 minutes on a rotating platform
439 followed by washing in PBS twice before staining. Fly strains used in our study are
440 listed in a Key Resources table.
441
442 ***Testis cell stage classification and measurements*.** Cells at an early stage of
443 development (stem cells and early-stage somatic and germline cells) were located in
444 the apical region of the testis, and were identified by their small and dense nuclei[120].
445 GSC were defined as Vasa-positive cells in direct contact with the hub; proliferating
446 GSC were identified as Vasa-positive cells in direct contact with the hub that were also
447 phospho-H3 positive. Cells in the testis region occupied by primary spermatocytes were
448 identified by their large cell size and decondensed chromosome staining occupying
449 three nuclear domains[120]. Spermatid bundles were identified by their condensed and
450 needle-shaped nuclei, which roughly corresponds to nuclei with protamine-based
451 chromatin[121]. Testis size was measured by quantifying the length of a line drawn
452 down the middle of a testis image; starting from the apical tip of the testis and ending
453 where the testis meets the seminal vesicle.
454
455 ***FLP-FRT clone induction.*** Adult males were collected at 3-5 days post-eclosion and
456 heat-shocked three times at 37°C with a 10 min rest period at room temperature
457 between heat shocks. After heat-shock, the flies were incubated at room temperature
458 until dissection.

Immunohistochemistry. Fixed samples were rinsed three times with blocking solution containing 0.2% bovine serum albumin (A4503, Sigma-Aldrich), 0.3% Triton-X in PBS, then blocked for 1 hr on a rotating platform at room temperature. During the incubation, the blocking solution was changed every 15 minutes. After blocking, the sample were resuspended in blocking solution with the appropriate concentration of primary antibody (see Key Resources table), and incubated overnight at 4°C. Samples were rinsed three times with blocking solution after removing primary antibody, and blocked for one hour on a rotating platform in blocking solution. Secondary antibody was applied in blocking solution and left on the rotating platform at room temperature for 40 min. The sample was rinsed with blocking solution three more times, and washed four times for 15 min per wash in blocking solution. Testis samples were resuspended in Vectashield mounting media with DAPI (H-1200-10, Vector Laboratory) or SlowFade Diamond mounting media (S36972, Thermo Fisher Scientific) prior to mounting.

Lipid droplet staining. Fixed testes were briefly permeabilized with 0.1% Triton-X in PBS for 5 min prior to applying phalloidin. For BODIPY staining, samples were suspended in PBS containing 10 µg/mL DAPI (2879083-5mg, PeproTech), 1:500 BODIPY 495/503 (Thermo Fisher Scientific D3922), and 1:1000 phalloidin iFluor647 (ab176759, Abcam) or 1:40 phalloidin TexasRed (T7471, Thermo Fisher Scientific). For staining with LipidTox Red, samples were suspended in PBS containing 10 µg/mL DAPI (2879083-5mg, PeproTech), 1:200 LipidTox Red (H34476, Thermo Fisher Scientific), and 1:1000 phalloidin iFluor647 (ab176759, Abcam). For staining free sterols, samples

were prepared as for BODIPY staining with 50 µg/mL filipin in place of BODIPY for 30 min. Samples were incubated on a rotating platform for 40 minutes at room temperature. After incubation, samples were washed twice with PBS, then resuspended in SlowFade Diamond mounting media (Thermo Fisher Scientific S36972) prior to mounting.

Image acquisition and processing. All images were acquired on a Leica SP5 confocal microscope system with 20X or 40X objectives and quantified with Fiji image analysis software[122].

Drosophila lipidomics. *Drosophila* extracts were prepared following the previously reported protocol[123]. Briefly, 10 *Drosophila* males (~10 mg) were weighed, 300 µL of ice-cold methanol/water mixture (9:1, v:v) was added to these males, and the samples were homogenized with glass beads using a bead beater (mini-beadbeater-16, BioSpec, Bartlesville, Ok, USA). Sample weight was used for sample normalization. Fly lysate was kept at -20°C for 4 hours for protein precipitation. Then, 900 µL of methyl tert-butyl ether was added and the solution was shaken for 5 min to extract lipids. To induce phase separation 285 µL of water was added, followed by centrifugation. The upper layer was separated, dried, and reconstituted in isopropanol/acetonitrile (1:1, v:v) for liquid chromatography-mass spectrometry (LC-MS) analysis. The volume of reconstitution solution was proportional to sample weight for normalization. Quality control (QC) samples were prepared by pooling 20 µL aliquot from each sample. The

method blank sample was prepared using an identical workflow but without adding *Drosophila*.

Drosophila extracts were analyzed on an UHR-QqTOF (Ultra-High Resolution Qq-Time-Of-Flight) mass spectrometry Impact II (Bruker Daltonics, Bremen, Germany) interfaced with an Agilent 1290 Infinity II LC Systems (Agilent Technologies, Santa Clara, CA, USA). LC separation was performed using a Waters reversed-phase (RP) UPLC Acquity BEH C18 Column (1.7 µm, 1.0 mm ×100 mm, 130 Å) (Milford, MA, USA) maintained at 30°C. For positive ion mode, the mobile phase A was 60% acetonitrile in water and the mobile phase B was 90% isopropanol in acetonitrile, both containing 5 mM ammonium formate (pH = 4.8, adjusted by formic acid). For negative ion mode, the mobile phase A was 60% acetonitrile in water and the mobile phase B was 90% isopropanol in acetonitrile, both containing 5 mM NH_4FA (pH = 9.8, adjusted by ammonium hydroxide). The LC gradient for positive and negative ion modes was set as follows: 0 min, 5% B; 8 min, 40% B; 14 min, 70% B; 20 min, 95% B; 23 min, 95% B; 24 min, 5% B; 33 min, 5% B. The flow rate was 0.1 mL/min. The injection volume was optimized to 2 µL in positive mode and 5 µL in negative mode using QC sample. The ESI source conditions were set as follows: dry gas temperature, 220 °C; dry gas flow, 7 L/min; nebulizer gas pressure, 1.6 bar; capillary voltage, 4500 V for positive mode and 3000 V for negative mode. The MS1 analysis was conducted using following parameters: mass range, 70-1000 m/z; spectrum type: centroid, calculated using maximum intensity; absolute intensity threshold: 250. Data-dependent MS/MS analysis parameters: collision energy: 16-30 eV; cycle time, 3 s; spectra rate: 4 Hz when intensity < 10^4 and 12 Hz when intensity > 10^5, linearly increased from 10^4 to 10^5.

External calibration was applied using sodium formate to ensure the m/z accuracy before sample analysis.

The raw LC-MS data were processed using MS-DIAL (ver. 4.38)[124]. The detailed MS-DIAL parameters are: MS1 tolerance, 0.01 Da; MS/MS tolerance, 0.05; mass slice width, 0.05 Da; smoothing method, linear weighted moving average; smoothing level, 3 scans; minimum peak width, 5 scans. Lipid features with high quantitative confidence were selected by the following criteria: retention time was within the gradient elution time (< 23 min); average intensity in QC samples is larger than 5-fold of the intensity in method blank sample. Lipid identification was performed by matching experimental precursor m/z, isotopic ratio and MS/MS spectrum against the LipidBlast libraries embedded in MS-DIAL. To improve the quantification accuracy, the measured MS signal intensities were corrected using serial diluted QC samples following the reported workflow[125].

Quantification and statistical analysis. All microscopy images were quantified using Fiji software[122]. For lipid droplet counts, a single optical slice through the middle of the testis containing the hub was used with the exception of FLP-FRT experiment where all lipid droplets within a GFP-negative cyst were counted (Figure 2I). All statistical analyses were done using R (obtained from https://cran.r-project.org). With exception of data concerning spatial distribution, and lipidomic data, Shapiro-Wilk test (via *shapiro.test* in base R) was used to assess normality of distribution prior to testing for significance. Kruskal-Wallis rank sum test (from the R package *coin*) and Dunn's test (from the R package *dunn.test*) were used in place of Welch two-sample t-test and

550 Tukey's multiple comparison test when the assumption of normality was not met. For
551 testing differences in variance between two populations, F-test (via *var.test* in base R)
552 was used. For testing differences in spatial distribution, two-sample Kolmogorov-
553 Smirnov test (via *ks.test* in base R) was used. All *p*-values are indicated in figures;
554 extremely small *p*-values are listed as $p<2.2 \times 10^{-16}$.
555

RESOURCE TABLE

REAGENT or RESOURCE	SOURCE	RESOURCE #
Antibodies		
Anti-Vasa (1:200)	Gift from Dr. R. Lehman, MIT	
Anti-Eya (1:50)	Developmental Studies Hybridoma Bank (DSHB)	eya10H6
Anti-zfh1 (1:1000)	Gift from Dr. J. Skeath, WUSTL	
Anti-boule (1:1000)	Gift from Dr. S. Wasserman, UCSD	
Anti-phospho-histone H3 (1:1000)	Millipore Sigma	05-1354
Experimental models: *Drosophila melanogaster*		
w^{1118}	Bloomington *Drosophila* stock center	3605
CantonS	Bloomington *Drosophila* stock center	64349
OregonR	Bloomington *Drosophila* stock center	25211
bmm^{1}	Gift from Dr. R. Kühnlein	
bmm^{rev}	Gift from Dr. R. Kühnlein	
mdy[Qx25], cn[1], bw[1]/CyO, l(2)DTS513[1]	Bloomington *Drosophila* stock center	5095
y[1],w[67c23];P{lacW}Cse1[k03802],mdy[k03902]/CyO	Bloomington *Drosophila* stock center	10536
w[1118];P{GD1749}v6367 (UAS-mdy-RNAi)	Vienna *Drosophila* resource center	6367

REAGENT or RESOURCE	SOURCE	RESOURCE #
nos-GAL4::VP16	Bloomington *Drosophila* stock center	7303
Tj-GAL4	Gift from Dr. D. Godt, University of Toronto	
c587-GAL4	Bloomington *Drosophila* stock center	67747
Bam-GFP	[40]	
bmm-GFP	Gift from Dr. K. Kamei[57]	
GFP-LD	Gift from Dr. M. Welte[36]	
P{neoFRT}82B, bmm[1]	This study	
P{neoFRT}82B, bmm[rev]	This study	
bam-GFP, bmm[1]	This study	
bam-GFP, bmm[rev]	This study	
Software and algorithms		
Fiji	https://imagej.net/software/fiji/	
R	https://cran.r-project.org	

SUPPLEMENTAL TABLE AND FILES

Supplemental table 1 – Table showing identified lipid species from untargeted lipidomic analysis.

Supplementary file 1 – Raw data and statistical outputs from Figure 1.

Supplementary file 2 – Raw data and statistical outputs from Figure 2 and Supplemental figure 2.

564 **Supplementary file 3** – Raw data and statistical outputs from Figure 3 and
565 Supplemental figure 3.
566 **Supplementary file 4** – Raw data and statistical outputs from Figure 4 and
567 Supplemental figure 4.
568
569 **SUPPLEMENTAL FIGURE LEGENDS**
570 **Supplemental Figure 1 related to Figure 1 – Cholesterol is absent from testis lipid**
571 **droplets.** (A) Testes stained with BODIPY (A) to detect neutral lipids and Filipin III (A')
572 to detect free cholesterol. Scale bars=50 μm.
573
574 **Supplemental Figure 2 related to Figure 2 – *bmm* mRNA levels during**
575 **spermatogenesis in germline and somatic lineages.** (A) Pseudotime trajectory of
576 germline (black line) based on single-cell RNA sequencing data[62]. Individual cells are
577 labeled according to the annotation within the data set. (B) Rolling average of
578 normalized *bmm* transcript counts in the germline along the trajectory shown in panel A
579 are plotted as a black line on the upper panel. Composition of cell types mapped on to
580 the trajectory at each time point is shown at the lower half of panel B. (C) Pseudotime
581 trajectory of the somatic cells (black line) based on publicly available single-cell RNA
582 sequencing data[62]. Individual cells are labeled according to the annotation within the
583 data set. (D) Rolling average of normalized *bmm* transcript counts in somatic cells
584 plotted as a black line along the trajectory shown in C (upper panel). Composition of cell
585 types mapped on to the trajectory at each time point (lower panel). (E-H)
586 Representative images of bmm^{rev} (E and F) and bmm^{1} (G and H) testes with somatic

587 over-expression of *GFP-LD* (*Tj-GAL4>UAS-GFP-LD*). Panel F and H contain magnified
588 images of the area indicated by the boxes in panel E and G, respectively. In bmm^{rev}
589 testes, LD were restricted to a region near the apical tip (E) of the testis in both somatic
590 (F–F''' arrows) and germline cells (F–F''' arrowheads). In bmm^{1} testes, LD were present
591 in both somatic (G–H arrows) and germline cells (G–H arrowheads), near the apical tip
592 of the testis in a region corresponding to early-stage germ cells and in the region
593 corresponding to spermatocytes. (E,G) Scale bars=50 μm; (F,H) scale bars=20 μm.
594
595 **Supplemental Figure 3 related to Figure 3 – Additional characterization of testis**
596 **development and spermatogenesis in animals lacking *bmm*.** (A) Testis size was
597 smaller in bmm^{1} mutant animals compared with bmm^{rev} controls at <24 hr post-eclosion
598 when raised at 25°C (A; Welch two-sample t-test). (B) The number of spermatid bundles
599 was significantly lower in bmm^{1} mutant animals compared with bmm^{rev} controls at <24
600 hr post-eclosion when raised at 25°C (Kruskal-Wallis rank sum test). (C) Testis size was
601 significantly smaller in bmm^{1} mutant males compared with bmm^{rev} control males at 14-
602 days post-eclosion (Welch two-sample t-test). (D) While the median number of
603 spermatid bundles was not significantly different between bmm^{1} mutant males and
604 bmm^{rev} control males at 14 days post-eclosion (Welch two-sample t-test), 8/27 bmm^{1}
605 testis had no spermatid bundles, a phenotype absent in age-matched bmm^{rev} males
606 (0/22) (p=0.0163, Pearson's Chi-squared test), suggesting a subtle defect is present.
607 (E) Food supplemented with 4% medium chain triglyceride (MCT), but not long chain
608 triglyceride (LCT), significantly increased testis length in bmm^{1} animals but had no effect
609 on this phenotype in bmm^{rev} control animals (one-way ANOVA with Tukey multiple

comparison test). (F) Food supplemented with 4% medium chain triglyceride significantly increased the number of spermatid bundles in *bmm*^{1} testes but had no effect on this phenotype in *bmm*^{rev} control animals (one-way ANOVA with Tukey multiple comparison test). (G) Representative images of *bmm*^{rev} (G–G') or *bmm*^{1} (G''–G''') testes stained for Fas3 (G and G'') and Vas (G' and G'''). Scale bars=25 μm. (H) Quantification of hub area in *bmm*^{rev} or *bmm*^{1} testes showed a significantly larger hub size in *bmm*^{1} testes (Welch two-sample t-test). (I) The number of germline stem cells (GSC) undergoing mitosis (phospho-histone H3^{+} GSC/total GSC) was not significantly different between *bmm*^{1} and *bmm*^{rev} testes (Kruskal-Wallis rank sum test). (J) The distance between the hub and the first Bam-GFP positive cyst (Figure 3H) was significantly higher in *bmm*^{1} testes than in *bmm*^{rev} testes (Welch two-sample t-test). (K) All *bmm*^{rev} testes and most *bmm*^{1} testes contained spermatids when raised at 25°C; however, the most advanced stage of spermatogenesis observed in the majority of *bmm*^{1} testes isolated from animals reared at 29°C was the spermatocyte stage. (L) Testes isolated from *bmm*^{1} animals showed a significantly smaller Boule-positive area than control testes (Welch two-sample t-test). (M) Testes isolated from *bmm*^{1} animals contain fewer individualization complexes than *bmm*^{rev} control testes (Kruskal-Wallis rank sum test). (N) Fewer waste bags were present in testes isolated from *bmm*^{1} animals compared with *bmm*^{rev} control testes (Kruskal-Wallis rank sum test).

Supplemental Figure 4 related to Figure 4 – Lipidomic analysis of animals lacking *bmm*. (A) Higher fold-changes of triglycerides in *bmm*^{1} animals were associated with less saturation in the acyl-groups (Kendall's rank correlation test). (B) Higher fold-

changes of triglycerides in *bmm*^{1} animals were associated with higher number of carbons in the acyl-groups (Kendall's rank correlation test). Each dot represents a single triglyceride species for panel B and C. (C) Volcano plot of identified lipids; monoglycerides shown in blue and diglycerides shown in orange. Many monoglycerides and diglycerides show increase in fold-change in *bmm*^{1} males. (D) The number of carbon and the degree of saturation of monoglycerides (MAG) and diglycerides (DAG) with significant changes in abundance between *bmm*^{1} and *bmm*^{rev} males. (E) Volcano plot of identified lipids; fatty acids shown in magenta and acyl-carnitine shown in green. Many fatty acids show an increase in fold-change while many acyl-carnitines show a decrease in fold-change in *bmm*^{1} males. (F) The number of carbon and the degree of saturation of fatty acids (FA) and acyl-carnitines (ACar) with significant changes in abundance between *bmm*^{1} and *bmm*^{rev} males. (G) Volcano plot of identified lipids; membrane lipids shown in yellow. (H) The number of carbon and the degree of saturation of membrane lipids with significant changes in abundance between *bmm*^{1} and *bmm*^{rev} males. For panel G and H, PC: phosphatidylcholine; PE: phosphatidylethanolamine; PI: phosphatidylinositol; LPC: lysophosphatidylcholine; LPE: lysophosphatidylethanolamine; SM: sphingomyelin; PG: phosphatidylglycerol. (I) Loss of *mdy* function rescued the elevated number of LD in *bmm*^{1} testes to control levels (one-way ANOVA with Tukey multiple comparison test). (J) Germline-specific loss of *mdy* in *bmm*^{1} animals did not reduce GSC numbers, but the variance in GSC number was significantly rescued (*nos-GAL4>+*; *bmm*^{1} vs *nos-GAL4>mdy RNAi*; *bmm*^{1}: p=4.5 × 10^{-5}; *+>mdy RNAi*; *bmm*^{1} vs *nos-GAL4>mdy RNAi*; *bmm*^{1}: p=0.0082 by F-test).

REFERENCES

1. Brill JA, Yildirim S, Fabian L. Phosphoinositide signaling in sperm development. Semin Cell Dev Biol. 2016;59: 2–9. doi:10.1016/j.semcdb.2016.06.010

2. Keber R, Rozman D, Horvat S. Sterols in spermatogenesis and sperm maturation. J Lipid Res. 2013;54: 20–33. doi:10.1194/jlr.R032326

3. Rato L, Alves MG, Socorro S, Duarte AI, Cavaco JE, Oliveira PF. Metabolic regulation is important for spermatogenesis. Nat Rev Urol. 2012;9: 330–338. doi:10.1038/nrurol.2012.77

4. Wang C, Huang X. Lipid metabolism and Drosophila sperm development. Sci China Life Sci. 2012;55: 35–40. doi:10.1007/s11427-012-4274-2

5. de Cuevas M, Matunis EL. The stem cell niche: lessons from the Drosophila testis. Dev Camb Engl. 2011;138: 2861–2869. doi:10.1242/dev.056242

6. Demarco RS, Eikenes ÅH, Haglund K, Jones DL. Investigating Spermatogenesis in Drosophila melanogaster. Methods San Diego Calif. 2014;68: 218–227. doi:10.1016/j.ymeth.2014.04.020

7. Fabian L, Brill JA. Drosophila spermiogenesis: Big things come from little packages. Spermatogenesis. 2012;2: 197–212. doi:10.4161/spmg.21798

8. Brill JA, Hime GR, Scharer-Schuksz M, Fuller MT. A phospholipid kinase regulates actin organization and intercellular bridge formation during germline cytokinesis. Development. 2000;127: 3855.

9. Giansanti MG, Bonaccorsi S, Kurek R, Farkas RM, Dimitri P, Fuller MT, et al. The Class I PITP Giotto Is Required for Drosophila Cytokinesis. Curr Biol. 2006;16: 195–201. doi:10.1016/j.cub.2005.12.011

10. Wong R, Hadjiyanni I, Wei H-C, Polevoy G, McBride R, Sem K-P, et al. PIP2 Hydrolysis and Calcium Release Are Required for Cytokinesis in Drosophila Spermatocytes. Curr Biol. 2005;15: 1401–1406. doi:10.1016/j.cub.2005.06.060

11. Wong R, Fabian L, Forer A, Brill JA. Phospholipase C and myosin light chain kinase inhibition define a common step in actin regulation during cytokinesis. BMC Cell Biol. 2007;8: 15. doi:10.1186/1471-2121-8-15

12. Amoyel M, Hillion K-H, Margolis SR, Bach EA. Somatic stem cell differentiation is regulated by PI3K/Tor signaling in response to local cues. Dev Camb Engl. 2016;143: 3914. doi:10.1242/dev.139782

13. Fairchild MJ, Islam F, Tanentzapf G. Identification of genetic networks that act in the somatic cells of the testis to mediate the developmental program of

spermatogenesis. PLOS Genet. 2017;13: e1007026. doi:10.1371/journal.pgen.1007026

14. Inaba M, Venkei ZG, Yamashita YM. The polarity protein Baz forms a platform for the centrosome orientation during asymmetric stem cell division in the Drosophila male germline. eLife. 2015;4: e04960. doi:10.7554/eLife.04960

15. Krahn MP, Klopfenstein DR, Fischer N, Wodarz A. Membrane Targeting of Bazooka/PAR-3 Is Mediated by Direct Binding to Phosphoinositide Lipids. Curr Biol. 2010;20: 636–642. doi:10.1016/j.cub.2010.01.065

16. Papagiannouli F, Berry CW, Fuller MT. The Dlg Module and Clathrin-Mediated Endocytosis Regulate EGFR Signaling and Cyst Cell-Germline Coordination in the Drosophila Testis. Stem Cell Rep. 2019;12: 1024–1040. doi:10.1016/j.stemcr.2019.03.008

17. Ueishi S, Shimizu H, Inoue YH. Male Germline Stem Cell Division and Spermatocyte Growth Require Insulin Signaling in Drosophila. Cell Struct Funct. 2009;34: 61–69. doi:10.1247/csf.08042

18. Phan VH, Herr DR, Panton D, Fyrst H, Saba JD, Harris GL. Disruption of Sphingolipid Metabolism Elicits Apoptosis-Associated Reproductive Defects in Drosophila. Dev Biol. 2007;309: 329–341. doi:10.1016/j.ydbio.2007.07.021

19. Steinhauer J, Gijón MA, Riekhof WR, Voelker DR, Murphy RC, Treisman JE. Drosophila Lysophospholipid Acyltransferases Are Specifically Required for Germ Cell Development. Mol Biol Cell. 2009;20: 5224–5235. doi:10.1091/mbc.e09-05-0382

20. Szafer-Glusman E, Giansanti MG, Nishihama R, Bolival B, Pringle J, Gatti M, et al. A Role for Very-Long-Chain Fatty Acids in Furrow Ingression during Cytokinesis in Drosophila Spermatocytes. Curr Biol. 2008;18: 1426–1431. doi:10.1016/j.cub.2008.08.061

21. Ben-David G, Miller E, Steinhauer J. Drosophila spermatid individualization is sensitive to temperature and fatty acid metabolism. Spermatogenesis. 2015;5. doi:10.1080/21565562.2015.1006089

22. Jung A, Hollmann M, Schafer MA. The fatty acid elongase NOA is necessary for viability and has a somatic role in Drosophila sperm development. J Cell Sci. 2007;120: 2924–2934. doi:10.1242/jcs.006551

23. Rabionet M, Bayerle A, Jennemann R, Heid H, Fuchser J, Marsching C, et al. Male meiotic cytokinesis requires ceramide synthase 3-dependent sphingolipids with unique membrane anchors. Hum Mol Genet. 2015;24: 4792–4808. doi:10.1093/hmg/ddv204

24. Santiago Valtierra FX, Peñalva DA, Luquez JM, Furland NE, Vásquez C, Reyes JG, et al. Elovl4 and Fa2h expression during rat spermatogenesis: a link to the very-long-chain PUFAs typical of germ cell sphingolipids. J Lipid Res. 2018;59: 1175–1189. doi:10.1194/jlr.M081885

25. Zadravec D, Tvrdik P, Guillou H, Haslam R, Kobayashi T, Napier JA, et al. ELOVL2 controls the level of n-6 28:5 and 30:5 fatty acids in testis, a prerequisite for male fertility and sperm maturation in mice. J Lipid Res. 2011;52: 245–255. doi:10.1194/jlr.M011346

26. Walther TC, Farese RV. Lipid Droplets and Cellular Lipid Metabolism. Annu Rev Biochem. 2012;81: 687–714. doi:10.1146/annurev-biochem-061009-102430

27. Wat LW, Chao C, Bartlett R, Buchanan JL, Millington JW, Chih HJ, et al. A role for triglyceride lipase brummer in the regulation of sex differences in Drosophila fat storage and breakdown. Hassan BA, editor. PLOS Biol. 2020;18: e3000595. doi:10.1371/journal.pbio.3000595

28. Thiele C, Spandl J. Cell biology of lipid droplets. Curr Opin Cell Biol. 2008;20: 378–385. doi:10.1016/j.ceb.2008.05.009

29. Bosma M. Lipid droplet dynamics in skeletal muscle. Exp Cell Res. 2016;340: 180–186. doi:10.1016/j.yexcr.2015.10.023

30. Grönke S, Müller G, Hirsch J, Fellert S, Andreou A, Haase T, et al. Dual Lipolytic Control of Body Fat Storage and Mobilization in Drosophila. PLOS Biol. 2007;5: e137. doi:10.1371/journal.pbio.0050137

31. Rambold AS, Cohen S, Lippincott-Schwartz J. Fatty Acid Trafficking in Starved Cells: Regulation by Lipid Droplet Lipolysis, Autophagy, and Mitochondrial Fusion Dynamics. Dev Cell. 2015;32: 678–692. doi:10.1016/j.devcel.2015.01.029

32. Dichlberger A, Schlager S, Maaninka K, Schneider WJ, Kovanen PT. Adipose triglyceride lipase regulates eicosanoid production in activated human mast cells. J Lipid Res. 2014;55: 2471–2478. doi:10.1194/jlr.M048553

33. Mitsche MA, Hobbs HH, Cohen JC. Patatin-like phospholipase domain–containing protein 3 promotes transfers of essential fatty acids from triglycerides to phospholipids in hepatic lipid droplets. J Biol Chem. 2018;293: 6958–6968. doi:10.1074/jbc.RA118.002333

34. Rajakumari S, Rajasekharan R, Daum G. Triacylglycerol lipolysis is linked to sphingolipid and phospholipid metabolism of the yeast Saccharomyces cerevisiae☆. Biochim Biophys Acta BBA - Mol Cell Biol Lipids. 2010;1801: 1314–1322. doi:10.1016/j.bbalip.2010.08.004

35. Schlager S, Goeritzer M, Jandl K, Frei R, Vujic N, Kolb D, et al. Adipose triglyceride lipase acts on neutrophil lipid droplets to regulate substrate availability for lipid

765 mediator synthesis. J Leukoc Biol. 2015;98: 837–850. doi:10.1189/jlb.3A0515-
766 206R

767 36. Zanghellini J, Natter K, Jungreuthmayer C, Thalhammer A, Kurat CF, Gogg-
768 Fassolter G, et al. Quantitative modeling of triacylglycerol homeostasis in yeast -
769 metabolic requirement for lipolysis to promote membrane lipid synthesis and
770 cellular growth: Triacylglycerol mobilization in yeast. FEBS J. 2008;275: 5552–
771 5563. doi:10.1111/j.1742-4658.2008.06681.x

772 37. Bailey AP, Koster G, Guillermier C, Hirst EMA, MacRae JI, Lechene CP, et al.
773 Antioxidant Role for Lipid Droplets in a Stem Cell Niche of Drosophila. Cell.
774 2015;163: 340–353. doi:10.1016/j.cell.2015.09.020

775 38. Liu L, MacKenzie KR, Putluri N, Maletić-Savatić M, Bellen HJ. The Glia-Neuron
776 Lactate Shuttle and Elevated ROS Promote Lipid Synthesis in Neurons and Lipid
777 Droplet Accumulation in Glia via APOE/D. Cell Metab. 2017;26: 719-737.e6.
778 doi:10.1016/j.cmet.2017.08.024

779 39. Nguyen TB, Louie SM, Daniele JR, Tran Q, Dillin A, Zoncu R, et al. DGAT1-
780 Dependent Lipid Droplet Biogenesis Protects Mitochondrial Function during
781 Starvation-Induced Autophagy. Dev Cell. 2017;42: 9-21.e5.
782 doi:10.1016/j.devcel.2017.06.003

783 40. Henne M. And three's a party: lysosomes, lipid droplets, and the ER in lipid
784 trafficking and cell homeostasis. Curr Opin Cell Biol. 2019;59: 40–49.
785 doi:10.1016/j.ceb.2019.02.011

786 41. Welte MA. Expanding Roles for Lipid Droplets. Curr Biol. 2015;25: R470–R481.
787 doi:10.1016/j.cub.2015.04.004

788 42. Casado ME, Pastor O, Mariscal P, Canfrán-Duque A, Martínez-Botas J, Kraemer
789 FB, et al. Hormone-sensitive lipase deficiency disturbs the fatty acid composition
790 of mouse testis. Prostaglandins Leukot Essent Fatty Acids. 2013;88: 227–233.
791 doi:10.1016/j.plefa.2012.12.005

792 43. El-Shehawi AM, El-Shazly S, Ahmed M, Alkafafy M, Sayed S, Farouk S, et al.
793 Transcriptome Analysis of Testis from HFD-Induced Obese Rats (Rattus
794 norvigicus) Indicated Predisposition for Male Infertility. Int J Mol Sci. 2020;21:
795 6493. doi:10.3390/ijms21186493

796 44. Wang W, Wei S, Li L, Su X, Du C, Li F, et al. Proteomic analysis of murine testes
797 lipid droplets. Sci Rep. 2015;5: 12070. doi:10.1038/srep12070

798 45. Bajpai M, Gupta G, Setty BS. Changes in carbohydrate metabolism of testicular
799 germ cells during meiosis in the rat. Eur J Endocrinol. 1998;138: 322–327.

46. Kerr JB, Kretser DMD. CYCLIC VARIATIONS IN SERTOLI CELL LIPID CONTENT THROUGHOUT THE SPERMATOGENIC CYCLE IN THE RAT. Reproduction. 1975;43: 1–8. doi:10.1530/jrf.0.0430001

47. Mori H, Christensen AK. Morphometric analysis of Leydig cells in the normal rat testis. J Cell Biol. 1980;84: 340–354. doi:10.1083/jcb.84.2.340

48. Paniagua R, Rodríguez MC, Nistal M, Fraile B, Amat P. Changes in the lipid inclusion/Sertoli cell cytoplasm area ratio during the cycle of the human seminiferous epithelium. Reproduction. 1987;80: 335–341. doi:10.1530/jrf.0.0800335

49. Demarco RS, Uyemura BS, D'Alterio C, Jones DL. Mitochondrial fusion regulates lipid homeostasis and stem cell maintenance in the Drosophila testis. Nat Cell Biol. 2019;21: 710–720. doi:10.1038/s41556-019-0332-3

50. Chen M, Wang H, Li X, Li N, Xu G, Meng Q. PLIN1 deficiency affects testicular gene expression at the meiotic stage in the first wave of spermatogenesis. Gene. 2014;543: 212–219. doi:10.1016/j.gene.2014.04.021

51. Hermo L, Chung S, Gregory M, Smith CE, Wang SP, El-Alfy M, et al. Alterations in the testis of hormone sensitive lipase-deficient mice is associated with decreased sperm counts, sperm motility, and fertility. Mol Reprod Dev. 2008;75: 565–577. doi:10.1002/mrd.20800

52. Masaki H, Kim N, Nakamura H, Kumasawa K, Kamata E, Hirano K, et al. Long-chain fatty acid triglyceride (TG) metabolism disorder impairs male fertility: a study using adipose triglyceride lipase deficient mice. MHR Basic Sci Reprod Med. 2017;23: 452–460. doi:10.1093/molehr/gax031

53. Freeman DA, Ascoli M. Studies on the source of cholesterol used for steroid biosynthesis in cultured Leydig tumor cells. J Biol Chem. 1982;257: 14231–14238.

54. Wang F, Chen Z, Ren X, Tian Y, Wang F, Liu C, et al. Hormone-sensitive lipase deficiency alters gene expression and cholesterol content of mouse testis. Reproduction. 2017;153: 175–185. doi:10.1530/REP-16-0484

55. de Cuevas M, Matunis EL. The stem cell niche: lessons from the Drosophila testis. Development. 2011;138: 2861–2869. doi:10.1242/dev.056242

56. Walther TC, Chung J, Jr RVF. Lipid Droplet Biogenesis. Annu Rev Cell Dev Biol. 2017;33: 491–510. doi:10.1146/annurev-cellbio-100616-060608

57. Boyle M, DiNardo S. Specification, migration and assembly of the somatic cells of the Drosophila gonad. Development. 1995;121: 1815–1825. doi:10.1242/dev.121.6.1815

58. Yu YV, Li Z, Rizzo NP, Einstein J, Welte MA. Targeting the motor regulator Klar to lipid droplets. BMC Cell Biol. 2011;12: 9. doi:10.1186/1471-2121-12-9

59. Leatherman JL, DiNardo S. Zfh-1 Controls Somatic Stem Cell Self-Renewal in the Drosophila Testis and Nonautonomously Influences Germline Stem Cell Self-Renewal. Cell Stem Cell. 2008;3: 44–54. doi:10.1016/j.stem.2008.05.001

60. Fabrizio JJ, Boyle M, DiNardo S. A somatic role for eyes absent (eya) and sine oculis (so) in drosophila spermatocyte development. Dev Biol. 2003;258: 117–128. doi:10.1016/S0012-1606(03)00127-1

61. Chen D, McKearin DM. A discrete transcriptional silencer in the bam gene determines asymmetric division of the Drosophila germline stem cell. Development. 2003;130: 1159–1170. doi:10.1242/dev.00325

62. Insco ML, Leon A, Tam CH, McKearin DM, Fuller MT. Accumulation of a differentiation regulator specifies transit amplifying division number in an adult stem cell lineage. Proc Natl Acad Sci U S A. 2009;106: 22311–22316. doi:10.1073/pnas.0912454106

63. Chen D, Wu C, Zhao S, Geng Q, Gao Y, Li X, et al. Three RNA Binding Proteins Form a Complex to Promote Differentiation of Germline Stem Cell Lineage in Drosophila. PLoS Genet. 2014;10. doi:10.1371/journal.pgen.1004797

64. Gonczy P, Matunis E, DiNardo S. bag-of-marbles and benign gonial cell neoplasm act in the germline to restrict proliferation during Drosophila spermatogenesis. Development. 1997;124: 4361–4371.

65. Athenstaedt K, Daum G. YMR313c/TGL3 Encodes a Novel Triacylglycerol Lipase Located in Lipid Particles of Saccharomyces cerevisiae*. J Biol Chem. 2003;278: 23317–23323. doi:10.1074/jbc.M302577200

66. Chitraju C, Trötzmüller M, Hartler J, Wolinski H, Thallinger GG, Haemmerle G, et al. The impact of genetic stress by ATGL deficiency on the lipidome of lipid droplets from murine hepatocytes. J Lipid Res. 2013;54: 2185–2194. doi:10.1194/jlr.M037952

67. Grönke S, Mildner A, Fellert S, Tennagels N, Petry S, Müller G, et al. Brummer lipase is an evolutionary conserved fat storage regulator in Drosophila. Cell Metab. 2005;1: 323–330. doi:10.1016/j.cmet.2005.04.003

68. Haemmerle G, Lass A, Zimmermann R, Gorkiewicz G, Meyer C, Rozman J, et al. Defective Lipolysis and Altered Energy Metabolism in Mice Lacking Adipose Triglyceride Lipase. Science. 2006;312: 734–737. doi:10.1126/science.1123965

69. Haemmerle G, Moustafa T, Woelkart G, Büttner S, Schmidt A, van de Weijer T, et al. ATGL-mediated fat catabolism regulates cardiac mitochondrial function via PPAR-α and PGC-1. Nat Med. 2011;17: 1076–1085. doi:10.1038/nm.2439

872 70. Huijsman E, van de Par C, Economou C, van der Poel C, Lynch GS, Schoiswohl G,
873 et al. Adipose triacylglycerol lipase deletion alters whole body energy metabolism
874 and impairs exercise performance in mice. Am J Physiol-Endocrinol Metab.
875 2009;297: E505–E513. doi:10.1152/ajpendo.00190.2009

876 71. Korbelius M, Vujic N, Sachdev V, Obrowsky S, Rainer S, Gottschalk B, et al.
877 ATGL/CGI-58-Dependent Hydrolysis of a Lipid Storage Pool in Murine
878 Enterocytes. Cell Rep. 2019;28: 1923-1934.e4. doi:10.1016/j.celrep.2019.07.030

879 72. Kurat CF, Natter K, Petschnigg J, Wolinski H, Scheuringer K, Scholz H, et al.
880 Obese Yeast: Triglyceride Lipolysis Is Functionally Conserved from Mammals to
881 Yeast *. J Biol Chem. 2006;281: 491–500. doi:10.1074/jbc.M508414200

882 73. Zimmermann R, Strauss JG, Haemmerle G, Schoiswohl G, Birner-Gruenberger R,
883 Riederer M, et al. Fat Mobilization in Adipose Tissue Is Promoted by Adipose
884 Triglyceride Lipase. Science. 2004;306: 1383–1386.
885 doi:10.1126/science.1100747

886 74. Attané C, Peyot M-L, Lussier R, Poursharifi P, Zhao S, Zhang D, et al. A beta cell
887 ATGL-lipolysis/adipose tissue axis controls energy homeostasis and body weight
888 via insulin secretion in mice. Diabetologia. 2016;59: 2654–2663.
889 doi:10.1007/s00125-016-4105-2

890 75. Lee JH, Kong J, Jang JY, Han JS, Ji Y, Lee J, et al. Lipid Droplet Protein LID-1
891 Mediates ATGL-1-Dependent Lipolysis during Fasting in Caenorhabditis elegans.
892 Mol Cell Biol. 2014;34: 4165–4176. doi:10.1128/MCB.00722-14

893 76. Tuohetahuntila M, Molenaar MR, Spee B, Brouwers JF, Houweling M, Vaandrager
894 AB, et al. ATGL and DGAT1 are involved in the turnover of newly synthesized
895 triacylglycerols in hepatic stellate cells. J Lipid Res. 2016;57: 1162–1174.
896 doi:10.1194/jlr.M066415

897 77. Men TT, Thanh DNV, Yamaguchi M, Suzuki T, Hattori G, Arii M, et al. A *Drosophila*
898 Model for Screening Antiobesity Agents. BioMed Res Int. 2016;2016: 1–10.
899 doi:10.1155/2016/6293163

900 78. Li H, Janssens J, Waegeneer MD, Kolluru SS, Davie K, Gardeux V, et al. Fly Cell
901 Atlas: a single-cell transcriptomic atlas of the adult fruit fly. bioRxiv; 2021. p.
902 2021.07.04.451050. doi:10.1101/2021.07.04.451050

903 79. Xu T, Rubin GM. Analysis of genetic mosaics in developing and adult Drosophila
904 tissues. Development. 1993;117: 1223–1237.

905 80. Kim N, Nakamura H, Masaki H, Kumasawa K, Hirano K, Kimura T. Effect of lipid
906 metabolism on male fertility. Biochem Biophys Res Commun. 2017;485: 686–692.
907 doi:10.1016/j.bbrc.2017.02.103

908 81. Lasko PF, Ashburner M. The product of the Drosophila gene vasa is very similar to
909 eukaryotic initiation factor-4A. Nature. 1988;335: 611–617. doi:10.1038/335611a0

910 82. Resende LPF, Boyle M, Tran D, Fellner T, Jones DL. Headcase Promotes Cell
911 Survival and Niche Maintenance in the Drosophila Testis. Bökel C, editor. PLoS
912 ONE. 2013;8: e68026. doi:10.1371/journal.pone.0068026

913 83. Kiger AA, White-Cooper H, Fuller MT. Somatic support cells restrict germline stem
914 cell self-renewal and promote differentiation. Nature. 2000;407: 750–754.
915 doi:10.1038/35037606

916 84. Lin TY, Viswanathan S, Wood C, Wilson PG, Wolf N, Fuller MT. Coordinate
917 developmental control of the meiotic cell cycle and spermatid differentiation in
918 Drosophila males. Development. 1996;122: 1331–1341.

919 85. Eichmann TO, Kumari M, Haas JT, Farese RV, Zimmermann R, Lass A, et al.
920 Studies on the substrate and stereo/regioselectivity of adipose triglyceride lipase,
921 hormone-sensitive lipase, and diacylglycerol-O-acyltransferases. J Biol Chem.
922 2012;287: 41446–41457. doi:10.1074/jbc.M112.400416

923 86. Schweiger M, Schreiber R, Haemmerle G, Lass A, Fledelius C, Jacobsen P, et al.
924 Adipose Triglyceride Lipase and Hormone-sensitive Lipase Are the Major
925 Enzymes in Adipose Tissue Triacylglycerol Catabolism *. J Biol Chem. 2006;281:
926 40236–40241. doi:10.1074/jbc.M608048200

927 87. Missaglia S, Maggi L, Mora M, Gibertini S, Blasevich F, Agostoni P, et al. Late
928 onset of neutral lipid storage disease due to novel PNPLA2 mutations causing
929 total loss of lipase activity in a patient with myopathy and slight cardiac
930 involvement. Neuromuscul Disord. 2017;27: 481–486.
931 doi:10.1016/j.nmd.2017.01.011

932 88. Williams ML, Coleman RA, Placezk D, Grunfeld C. Neutral lipid storage disease: a
933 possible functional defect in phospholipid-linked triacylglycerol metabolism.
934 Biochim Biophys Acta BBA - Mol Basis Dis. 1991;1096: 162–169.
935 doi:10.1016/0925-4439(91)90055-E

936 89. Yang L, Liang J, Lam SM, Yavuz A, Shui G, Ding M, et al. Neuronal lipolysis
937 participates in PUFA-mediated neural function and neurodegeneration. EMBO
938 Rep. 2020;21. doi:10.15252/embr.202050214

939 90. Nazario-Yepiz NO, Fernández Sobaberas J, Lyman R, Campbell MR, Shankar V,
940 Anholt RRH, et al. Physiological and metabolomic consequences of reduced
941 expression of the Drosophila brummer triglyceride Lipase. Melkani GC, editor.
942 PLOS ONE. 2021;16: e0255198. doi:10.1371/journal.pone.0255198

943 91. Giedt MS, Thomalla JM, Johnson MR, Lai ZW, Tootle TL, Welte MA. Adipose
944 triglyceride lipase promotes prostaglandin-dependent actin remodeling by

regulating substrate release from lipid droplets. Cell Biology; 2021 Aug. doi:10.1101/2021.08.02.454724

92. Beller M, Bulankina AV, Hsiao H-H, Urlaub H, Jäckle H, Kühnlein RP. PERILIPIN-Dependent Control of Lipid Droplet Structure and Fat Storage in Drosophila. Cell Metab. 2010;12: 521–532. doi:10.1016/j.cmet.2010.10.001

93. Buszczak M, Lu X, Segraves WA, Chang TY, Cooley L. Mutations in the midway Gene Disrupt a Drosophila Acyl Coenzyme A: Diacylglycerol Acyltransferase. Genetics. 2002;160: 1511–1518.

94. Martínez BA, Hoyle RG, Yeudall S, Granade ME, Harris TE, Castle JD, et al. Innate immune signaling in Drosophila shifts anabolic lipid metabolism from triglyceride storage to phospholipid synthesis to support immune function. PLOS Genet. 2020;16: e1009192. doi:10.1371/journal.pgen.1009192

95. Freeman DA, Ascoli M. Studies on the source of cholesterol used for steroid biosynthesis in cultured Leydig tumor cells. J Biol Chem. 1982;257: 14231–14238.

96. Wang F, Chen Z, Ren X, Tian Y, Wang F, Liu C, et al. Hormone-sensitive lipase deficiency alters gene expression and cholesterol content of mouse testis. Reproduction. 2017;153: 175–185. doi:10.1530/REP-16-0484

97. Walther TC, Farese RV. Lipid droplets and cellular lipid metabolism. Annu Rev Biochem. 2012;81: 687–714. doi:10.1146/annurev-biochem-061009-102430

98. Olzmann JA, Carvalho P. Dynamics and functions of lipid droplets. Nat Rev Mol Cell Biol. 2019;20: 137–155. doi:10.1038/s41580-018-0085-z

99. Birse RT, Choi J, Reardon K, Rodriguez J, Graham S, Diop S, et al. High-fat-diet-induced obesity and heart dysfunction are regulated by the TOR pathway in Drosophila. Cell Metab. 2010;12: 533–44. doi:10.1016/j.cmet.2010.09.014

100. Molaei M, Vandehoef C, Karpac J. NF-κB Shapes Metabolic Adaptation by Attenuating Foxo-Mediated Lipolysis in Drosophila. Dev Cell. 2019;49: 802-810.e6. doi:10.1016/j.devcel.2019.04.009

101. Alic N, Andrews TD, Giannakou ME, Papatheodorou I, Slack C, Hoddinott MP, et al. Genome-wide dFOXO targets and topology of the transcriptomic response to stress and insulin signalling. Mol Syst Biol. 2011;7: 502. doi:10.1038/msb.2011.36

102. Junger MA, Rintelen F, Stocker H, Wasserman JD, Vegh M, Radimerski T, et al. The Drosophila forkhead transcription factor FOXO mediates the reduction in cell number associated with reduced insulin signaling. J Biol. 2003;2: 20. doi:10.1186/1475-4924-2-20

103. Zinke I, Schutz CS, Katzenberger JD, Bauer M, Pankratz MJ. Nutrient control of gene expression in Drosophila: microarray analysis of starvation and sugar-dependent response. EMBO J. 2002;21: 6162–73.

104. Puig O, Tjian R. Transcriptional feedback control of insulin receptor by dFOXO/FOXO1. Genes Dev. 2005;19: 2435–2446. doi:10.1101/gad.1340505

105. Kang P, Chang K, Liu Y, Bouska M, Birnbaum A, Karashchuk G, et al. Drosophila Kruppel homolog 1 represses lipolysis through interaction with dFOXO. Sci Rep. 2017;7: 16369. doi:10.1038/s41598-017-16638-1

106. Bartz R, Zehmer JK, Zhu M, Chen Y, Serrero G, Zhao Y, et al. Dynamic activity of lipid droplets: protein phosphorylation and GTP-mediated protein translocation. J Proteome Res. 2007;6: 3256–3265. doi:10.1021/pr070158j

107. Pagnon J, Matzaris M, Stark R, Meex RCR, Macaulay SL, Brown W, et al. Identification and functional characterization of protein kinase A phosphorylation sites in the major lipolytic protein, adipose triglyceride lipase. Endocrinology. 2012;153: 4278–4289. doi:10.1210/en.2012-1127

108. Narbonne P, Roy R. Caenorhabditis elegans dauers need LKB1/AMPK to ration lipid reserves and ensure long-term survival. Nature. 2009;457: 210–214. doi:10.1038/nature07536

109. Ahmadian M, Abbott MJ, Tang T, Hudak CSS, Kim Y, Bruss M, et al. Desnutrin/ATGL is regulated by AMPK and is required for a brown adipose phenotype. Cell Metab. 2011;13: 739–748. doi:10.1016/j.cmet.2011.05.002

110. Amoyel M, Hillion K-H, Margolis SR, Bach EA. Somatic stem cell differentiation is regulated by PI3K/Tor signaling in response to local cues. Dev Camb Engl. 2016;143: 3914–3925. doi:10.1242/dev.139782

111. Amoyel M, Simons BD, Bach EA. Neutral competition of stem cells is skewed by proliferative changes downstream of Hh and Hpo. EMBO J. 2014;33: 2295–2313. doi:10.15252/embj.201387500

112. Ueishi S, Shimizu H, H. Inoue Y. Male Germline Stem Cell Division and Spermatocyte Growth Require Insulin Signaling in Drosophila. Cell Struct Funct. 2009;34: 61–69. doi:10.1247/csf.08042

113. Hof-Michel S, Cigoja L, Huhn S, Bökel C. Innate immune signalling drives loser cell elimination during stem cell competition in the *Drosophila* testis. Developmental Biology; 2020 Mar. doi:10.1101/2020.03.05.979161

114. Couderc J-L, Richard G, Vachias C, Mirouse V. Drosophila LKB1 is required for the assembly of the polarized actin structure that allows spermatid individualization. White-Cooper H, editor. PLOS ONE. 2017;12: e0182279. doi:10.1371/journal.pone.0182279

115. Steinhauer J, Statman B, Fagan JK, Borck J, Surabhi S, Yarikipati P, et al. Combover interacts with the axonemal component Rsp3 and is required for Drosophila sperm individualization. Dev Camb Engl. 2019;146: dev179275. doi:10.1242/dev.179275

116. Tartarin P, Guibert E, Touré A, Ouiste C, Leclerc J, Sanz N, et al. Inactivation of AMPKα1 induces asthenozoospermia and alters spermatozoa morphology. Endocrinology. 2012;153: 3468–3481. doi:10.1210/en.2011-1911

117. Martin-Hidalgo D, Hurtado de Llera A, Calle-Guisado V, Gonzalez-Fernandez L, Garcia-Marin L, Bragado MJ. AMPK Function in Mammalian Spermatozoa. Int J Mol Sci. 2018;19: 3293. doi:10.3390/ijms19113293

118. Pitetti J-L, Calvel P, Zimmermann C, Conne B, Papaioannou MD, Aubry F, et al. An Essential Role for Insulin and IGF1 Receptors in Regulating Sertoli Cell Proliferation, Testis Size, and FSH Action in Mice. Mol Endocrinol. 2013;27: 814–827. doi:10.1210/me.2012-1258

119. Thurmond J, Goodman JL, Strelets VB, Attrill H, Gramates LS, Marygold SJ, et al. FlyBase 2.0: the next generation. Nucleic Acids Res. 2018;47: D759–D765. doi:10.1093/nar/gky1003

120. White-Cooper H. Spermatogenesis. In: Henderson DS, editor. Drosophila Cytogenetics Protocols. Totowa, NJ: Humana Press; 2004. pp. 45–75. doi:10.1385/1-59259-665-7:45

121. Fabian L, Brill JA. Drosophila spermiogenesis. Spermatogenesis. 2012;2: 197–212. doi:10.4161/spmg.21798

122. Schindelin J, Arganda-Carreras I, Frise E, Kaynig V, Longair M, Pietzsch T, et al. Fiji: an open-source platform for biological-image analysis. Nat Methods. 2012;9: 676–682. doi:10.1038/nmeth.2019

123. Yu H, Villanueva N, Bittar T, Arsenault E, Labonté B, Huan T. Parallel metabolomics and lipidomics enables the comprehensive study of mouse brain regional metabolite and lipid patterns. Anal Chim Acta. 2020;1136: 168–177. doi:10.1016/j.aca.2020.09.051

124. Tsugawa H, Cajka T, Kind T, Ma Y, Higgins B, Ikeda K, et al. MS-DIAL: data-independent MS/MS deconvolution for comprehensive metabolome analysis. Nat Methods. 2015;12: 523–526. doi:10.1038/nmeth.3393

125. Yu H, Huan T. Patterned Signal Ratio Biases in Mass Spectrometry-Based Quantitative Metabolomics. Anal Chem. 2021;93: 2254–2262. doi:10.1021/acs.analchem.0c04113

1052
1053

1054

Figure 1 – Lipid droplets are present in early-stage somatic and germline cells.

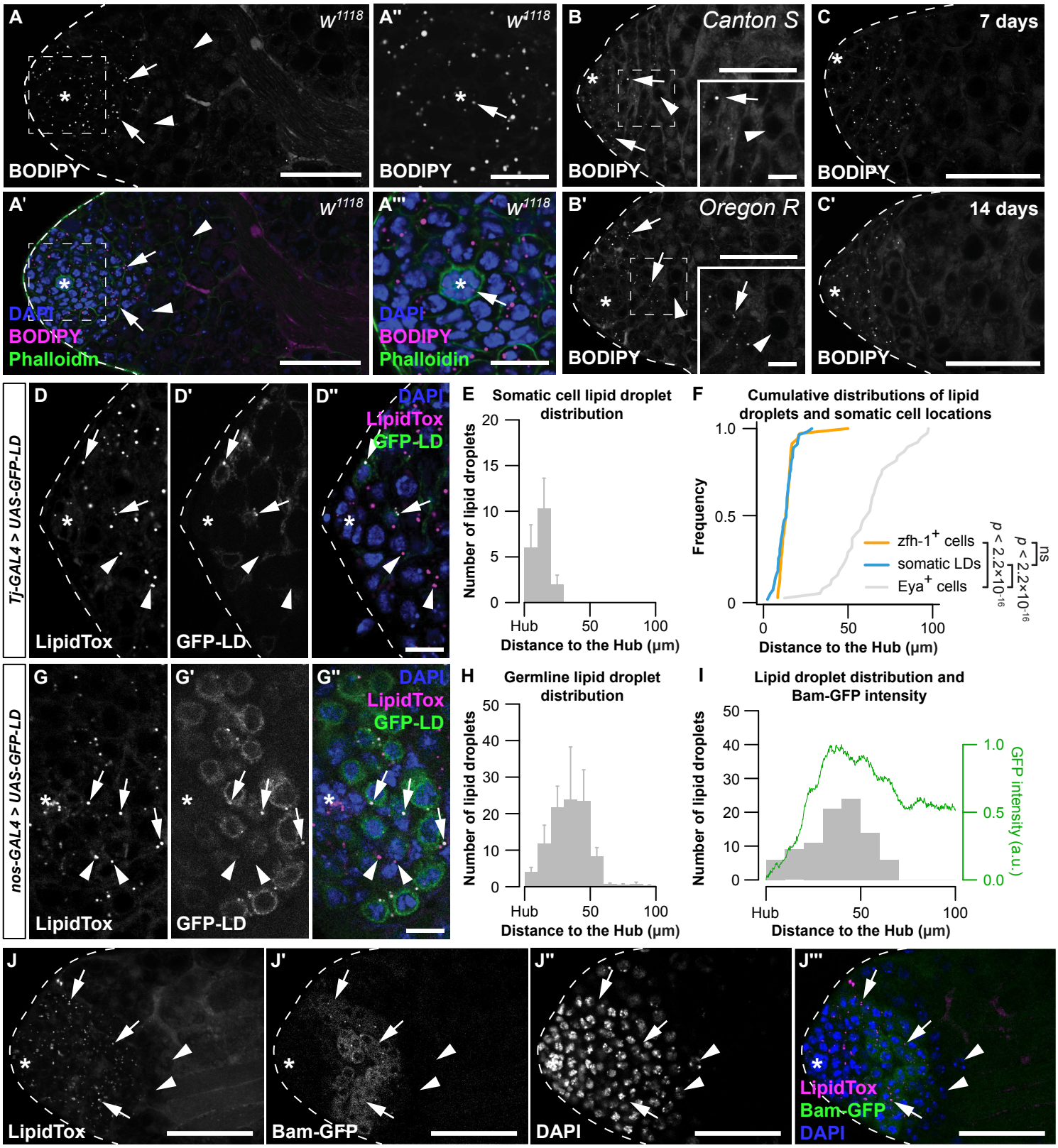

Figure 2 — *brummer* regulates testis lipid droplets in a cell-autonomous manner

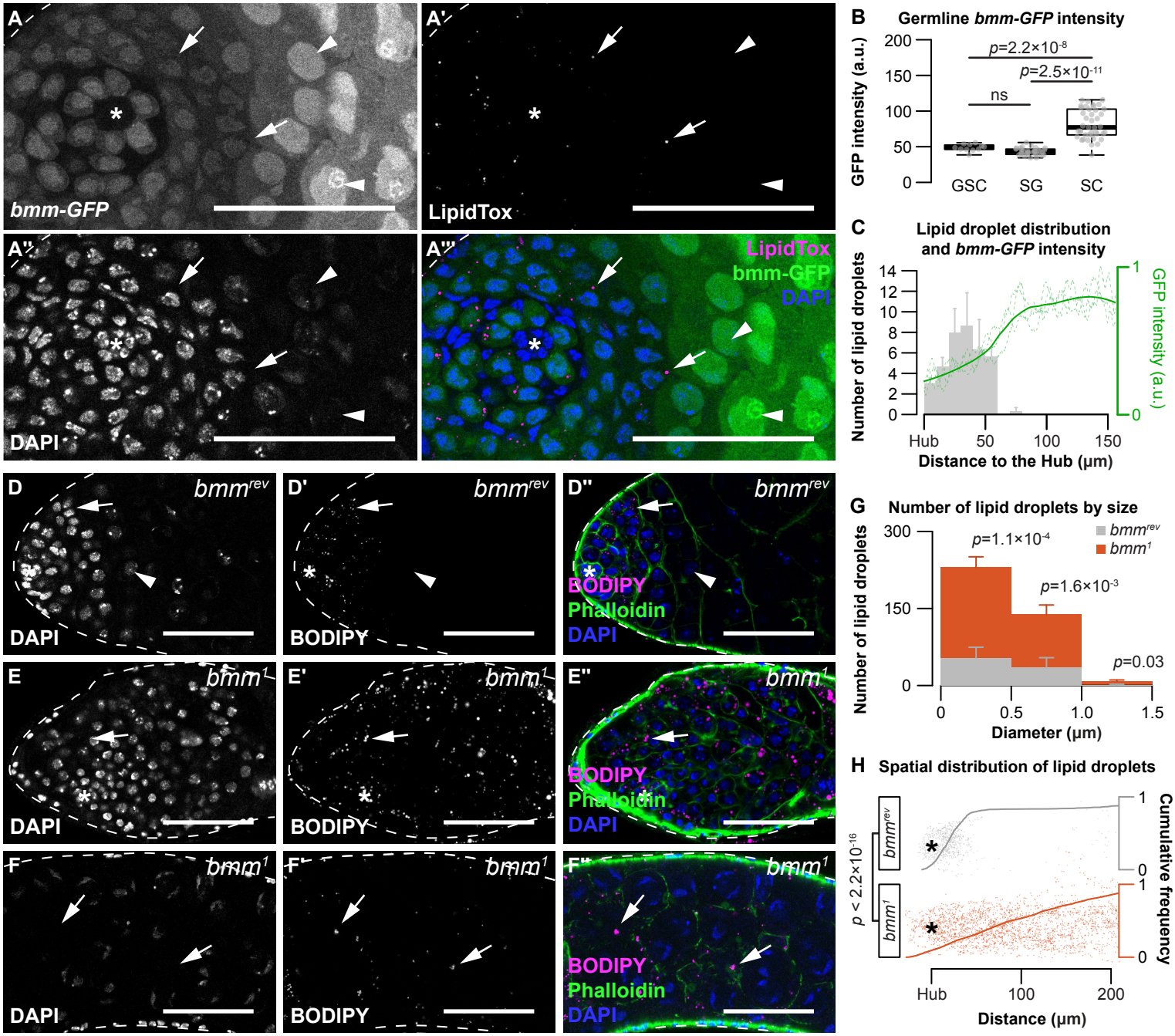

Figure 3. A cell-autonomous role of *brummer* in regulating spermatogenesis.

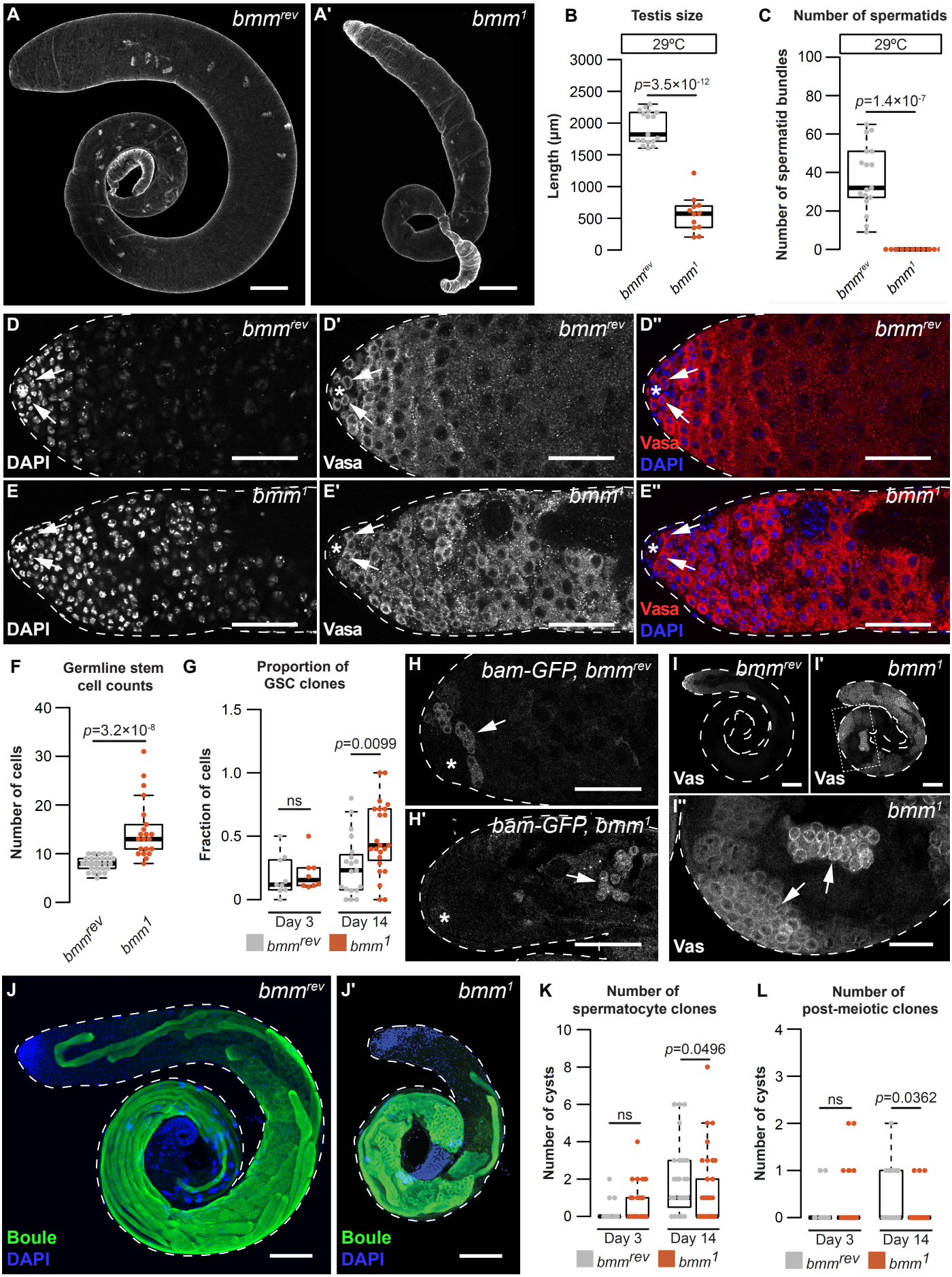

Figure 4. Loss of *brummer* disrupts triglyceride homeostasis and leads to spermatogenic defects.

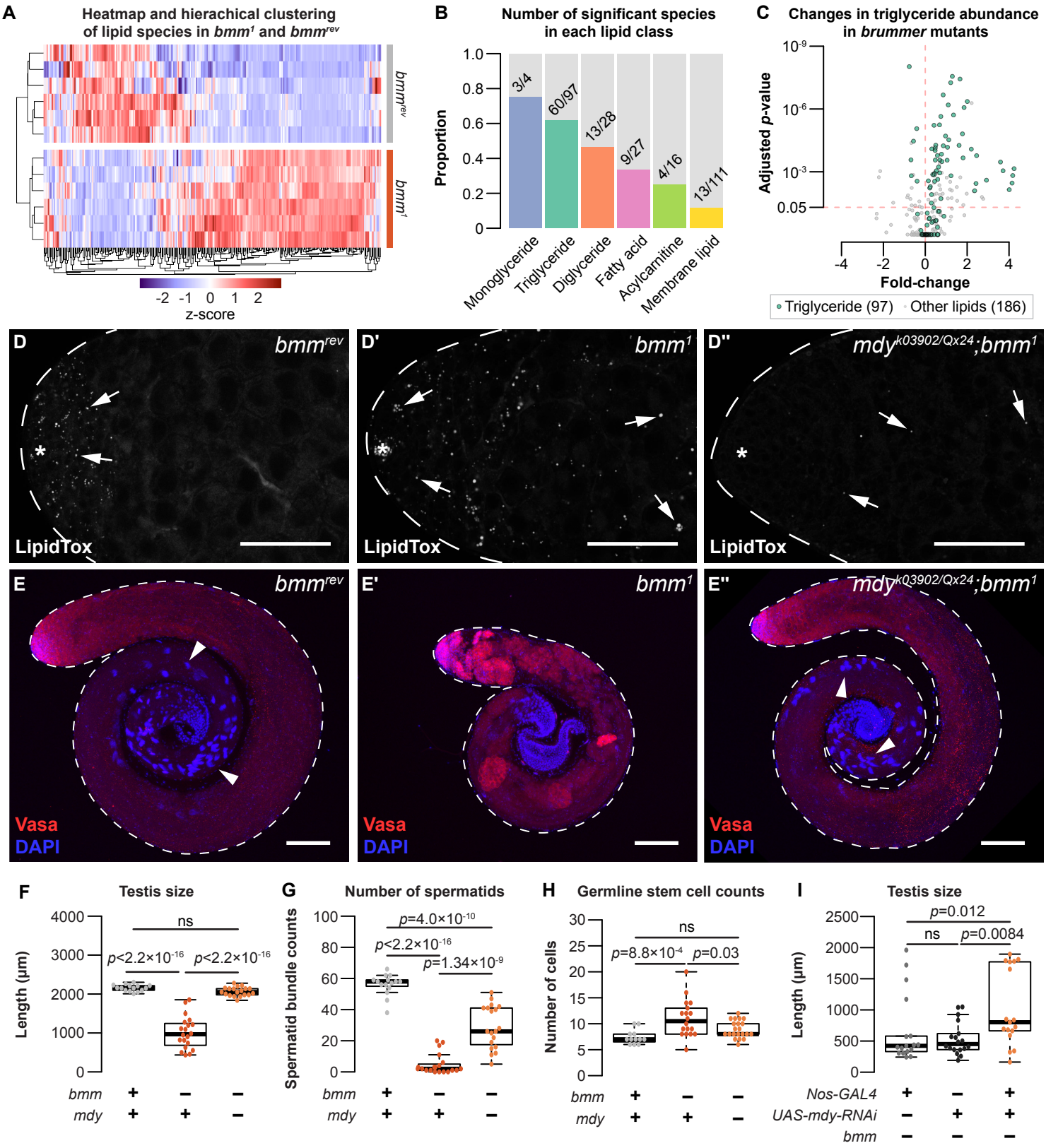

Supplemental Figure 1 – Cholesterol is absent from testis lipid droplets

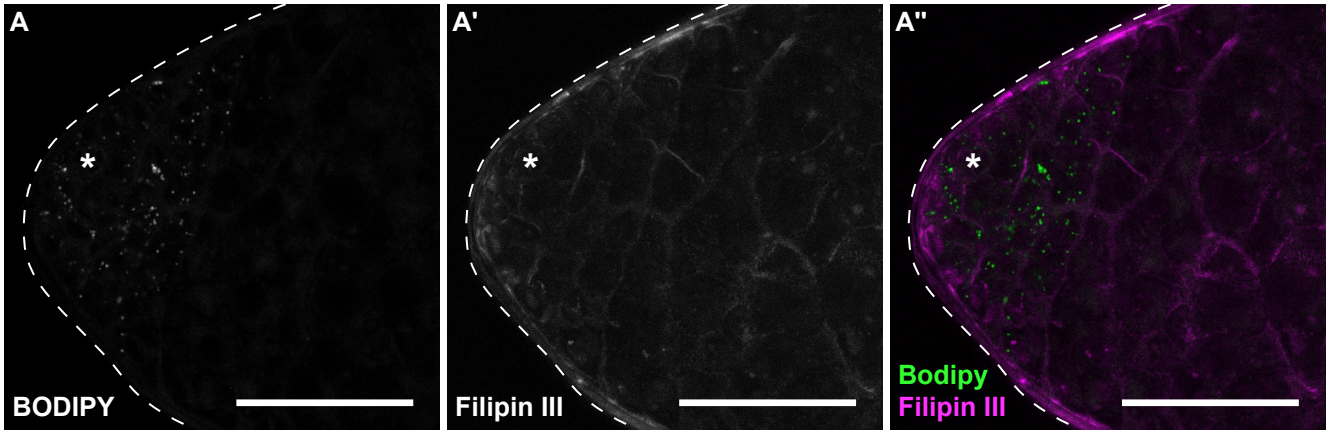

Supplemental Figure 2 – *brummer* regulates testis lipid droplets in a cell-autonomous manner

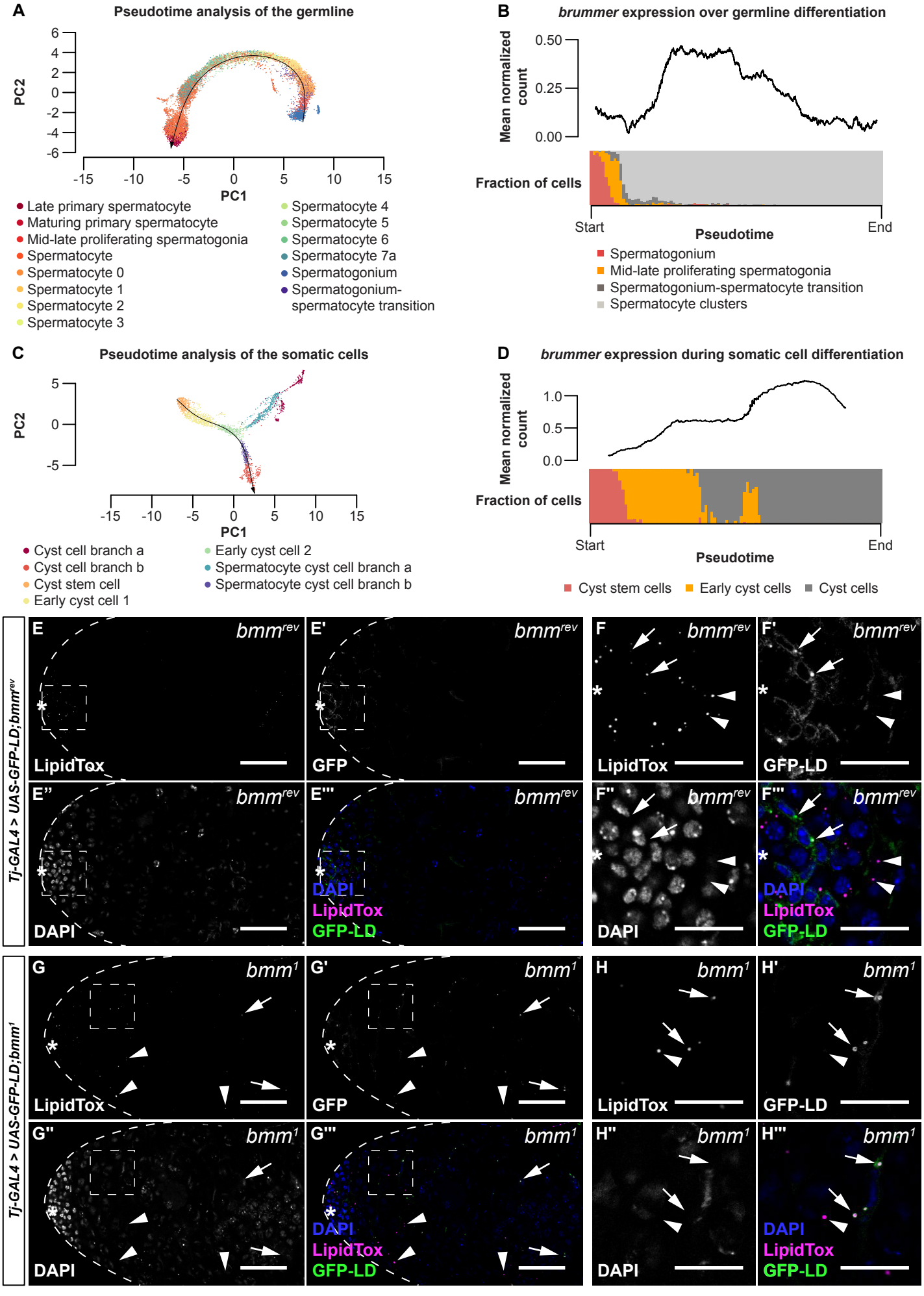

Supplemental Figure 3 – Additional characterization of testis development and spermatogenesis in animals lacking *brummer*.

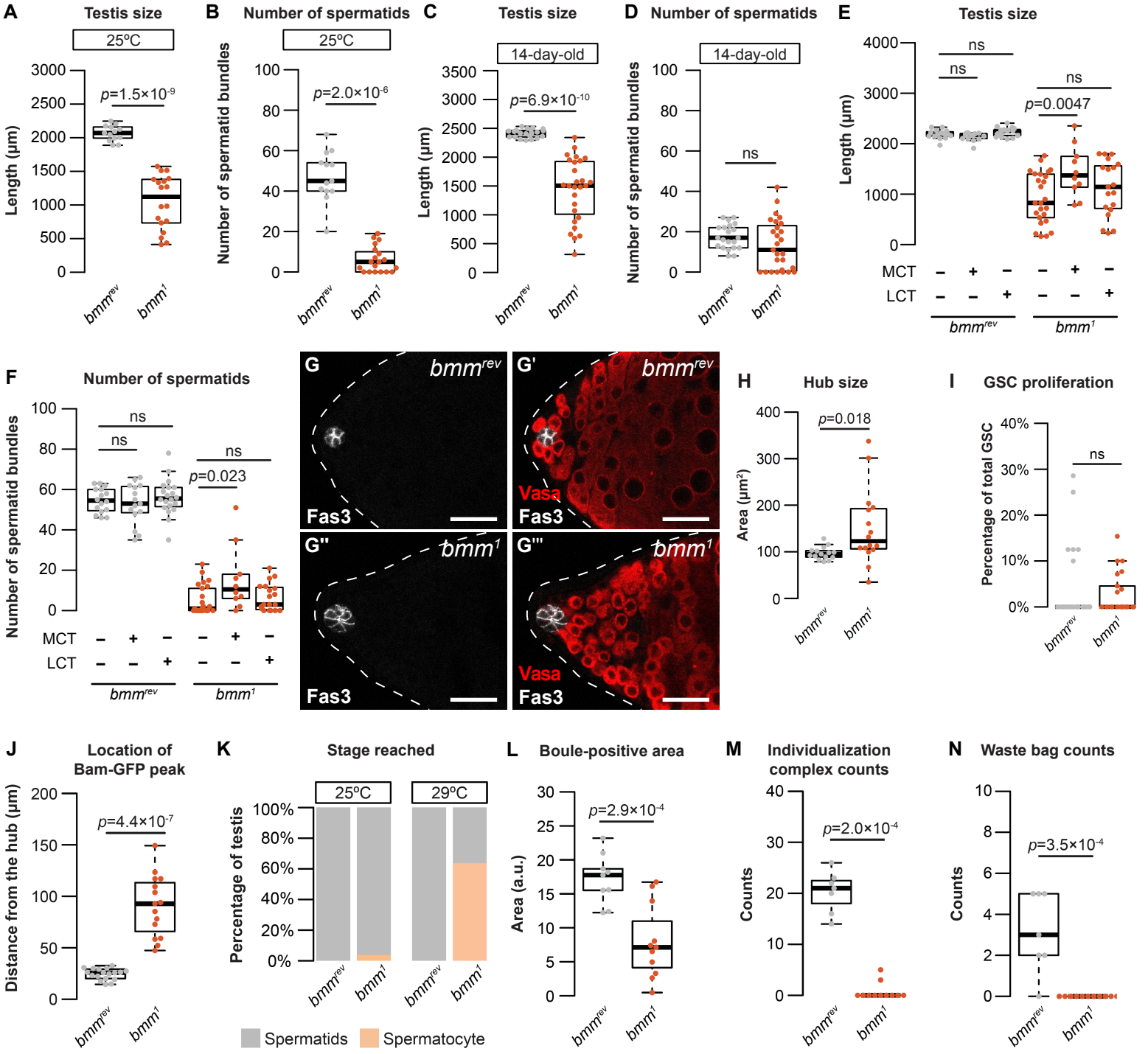

Supplemental Figure 4 – Lipidomic analysis of animals lacking *brummer*